National Institute of Electricity and Electronics
INELEC - BOUMERDES

DEPARTMENT OF RESEARCH

THESIS

Presented in partial fulfilment of the requirements of the

DEGREE OF MAGISTER

in Electronic System Engineering

by

Mahmoud AFFANE

Multi-Dimensional Quasi-Static Analysis of MIC's and MMIC's

Defended on July 17, 1994 before the jury:

President: Dr B. HARAOUBIA (MC - USTHB).
Members: Dr H. BOURDOUCEN (MC - INELEC).
Dr M. ATTARI (CC - USTHB).
Dr M. DJEDDI (CC - INELEC).

Registration number: 03/94

To my mother.

To my wife.

To Amel and Choukri.

Aknowledgments

I would like to express my deep and sincere appreciations to my supervisor Dr H. BOURDOUCEN (MC - INELEC) for his guidance and help.

My sincere gratitude is due to the president of the jury Dr B. HARAOUBIA (MC - USTHB) and the members of the jury Dr M. ATTARI (CC - USTHB) and Dr M. DJEDDI (CC - INELEC) for their acceptance.

My thinks are due to A. Ouadi, A. Zitouni, M. Dehmas, H. Bentarzi and R. Boucheta for their help and contribution to the realization of this project.

I would like to thank all the INELEC staff -post graduate department in particular- for their support and guidance; without forgetting the staff of the library, the computer center and the reprography room for their highly appreciated help.

ABSTRACT

Microwave Integrated Circuits (MIC's) and High Frequency Digital Circuits (HFDC's) have reached a high degree of complexity arising essentially from increasing integrations levels and the use of multilayer parallel and crossing microstrip interconnections as well as arbitrary shaped metalizations on different interfaces of isotropic and anisotropic dielectric substrates.

Presently, taking into account the constraints in MIC's dimensions, CAD tools are necessary to optimize the coupling capacitances and inductances between conductors as well as the fringing capacitances occuring on the metalization discontinuities.

In our work, we have applied the Method of Lines to develop a software program to analyze, in quasi-static approach, some microwave structure and components. The Method of Lines was selected because of its numerous advantages among them the suitability to deal with complex microwave structures, no relative convergence problem, low memory space requirement and no spurious physical results.

We have extended the application of this method to two layers of parallel conductors, isolated crossing conductors as well as rectangular and open-end microstrips with vanishing thickness deposited on anisotropic dielectric substrates of Sapphire. The results agree well with theoretical predictions and published data where more complex mathematical approaches have been used.

Also, some of the three-dimensional problems have been

analyzed in quasi-static with an emphasis on the anisotropy of Sapphire which is prefered for its various known advantages in microwave integrated circuits.

CONTENT

CHAPTER2

THE METHOD OF LINES APPLIED TO ONE-DIMENSIONAL DISCRETIZATION

CHAPTER3

THE METHOD OF LINES APPLIED TO THREE-DIMENSIONAL PROBLEMS

CHAPTER 4

RESULTS AND DISCUSSIONS

INTRODUCTION :

In Microwave Integrated Circuits (MIC's), microstrip components are the essential elements regarding their technological process advantages. They are involved in the form of lumped elements having all types of discontinuities and in the form of multilayer parallel and/or crossing interconnections relating the microwave active and passive devices [1],[2].

In reality, even for a simple microstrip structure, the analysis is made very complicated because of the singular behaviour of the electric and magnetic fields at the air-dielectric interface and particularly at the conductor edges and corners. We can imagine the analysis complications encountered with the microwave and high speed digital integrated circuits fabricated during the two last decades and involving higher integration, inhomogeneous, anisotropic and gyromagnetic dielectric substrates. All these technological needs and constraints, increasing with circuits complexity, have stimulated, during many decades, the development of various numerical and pseudo-numerical analysis techniques that are strengthing numerous CAD tools. Part of these methods are based on the quasi-static approach which is valid in the low gigahertz region and, even more, provides design guidance and serves as a basis for solution of the full-wave propagation problem. The quasi-static analysis is necessary knowing that a full-wave analysis of a complete monolithic integrated circuit will not be possible in the immediate

future with acceptable numerical expense [3].

With this analysis approach, multiconductor transmission lines in multilayer media have been investigated by means of Green's function techniques [4], conformal mapping [5], variational method [6], Fourier transform method [7], Fourier integral method [8], and generalized spectral domain analysis [9]. For three-dimensional problems, caused mainly by arbitrary shaped conductors and discontinuities, different Green's function methods have been applied :

- Galerkin's method in spectral domain [10].
- Matrix inversion method [11].
- Integral equation technique [12].

All the precited methods use generally, either Green's functions that are not easy to formulate for complex structures or expansion functions whose truncations may rise convergence problems due to the fields singular behaviour at conductors and dielectric discontinuities.

A method, recently applied to MIC problems analysis, called in mathematical literature "the method of lines (MoL)", has been used to calculate microwave elements, in 1980, by Shulz and Pregla [13]. This method is very efficient for the analysis of planar and quasi-planar microwave and optical waveguide structures. The MoL has been extended to three-dimensional problems, in 1984, by Worm and Pregla [14], applied, in quasi-static, firstly to parallel multiconductor systems, by Diestel in 1987 [15], and later to isolated crossing conductors, by Veit et al in 1990 [16]. This method presents numerous advantages:

_ easy mathematical formulation.

_ high accuracy with little numerical effort, unlike finite difference method.

_ suitability to deal with complex two and three-dimensional problems.

_ no relative convergence problem.

_ no spurious solution, unlike finite element method.

_ no necessity of prior knowledge about fields, unlike spectral domain method.

In quasi-static approach, with the method of lines, Laplace's equation is solved analytically in the dielectric subtrates by discretizing one space variable for constant cross-section structures and two variables for arbitrary shaped conductors. The last space variable perpendicular to the dielectric interfaces is kept continuous regarding the uniformity of the dielectric substrates. Hence, an analytical expression is found for the electric potential on each discretization line, by applying the continuity conditions to the dielectric interfaces and the boundary conditions to the shielding enclosure. The discretization yields vectors of electric potentials and charge densities that are related by a matrix that is reduced to the elements corresponding to the conductors and inverted to obtain the conductors microcapacitance matrix. Finally, by summing the appropriate terms, the lumped capacitance is determined in the case of arbitrary shaped conductors; while the lineique capacitances are determined for constant cross-section structures.

In our work, we have applied the method of lines in

quasi-static approach to analyze some MIC's problems. We have used this method, assuming infinitesimal thickness conductors, to calculate the microstrip TEM parameters (lineique capacitance, impedance and effective permitivity), to study the effects of the shielding enclosure on a microstrip lineique capacitance, and to determine the Maxwellian capacitance matrix of two arrays of parallel conductors separated by two dielectric substrates. We have investigated the effects of the strip width to substrate thickness ratio on the capacitances of a microstrip, two isolated crossing conductors and some microstrip discontinuities. The investigations have been done considering different dielectric permitivities with an emphasis on the anisotropy effects of the Sapphire dielectric.

In chapter one, an overview is given about the evolution of MIC's, focusing on the microstrip interconnections, discontinuities and quasi-static methods used to analyze them.

In chapter two the method of lines with one-dimensional discretization is presented with a detailed analysis of two multiconductor arrays separated by two dielectric substrates. Then, clarifications are given about the positioning of the discretization lines on and between the conductors and near the shielding walls. Finally, an illustrative example is given about the calculation of the capacitance of a microstrip with all the steps and intermediate numerical results as well as the description of the software program.

In chapter three, this method is applied with two-dimensional discretization to analyze three-dimensional

problems, namely, the coupling capacitance between two isolated crossing conductors, microstrip sections and discontinuities. Then, the application of this method, to anisotropic dielectrics, is outlined. Finally, the software program is described.

In chapter four, the results obtained with the semi-analytical method of lines are compared to those reached with other analytical and numerical techniques in the cases of two and three dimensional problems; with an emphasis on the anisotropy effects of Sapphire.

Finally, the possible and necessary extensions of the application of the MoL to more MIC's and MMIC's structures and components are summarized in a conclusion.

CHAPTER 1

GENERALITIES:

In this chapter, the history of the development of MIC components is given as well as the analysis methods employed for such elements which are mainly: microstrip transmission lines and microstrip sections with various discontinuities [17].

1-1 Evolution of microwave integrated circuits:

1-1-1 Concept of lumped parameters:

Low frequency electronic circuits are generally composed of lumped elements, active devices and interconnections between the various passive elements and active devices. Typical lumped elements are capacitors, inductors and resistors whose values are assumed to be concentrated in the corresponding elements. This assumption is valid for low frequencies at which the dimensions of the lumped elements are much smaller than the wavelength under consideration. However, at higher frequencies, the components dimensions and wavelength become comparable and the apparition of stray elements begins under the form of inductance between the capacitors plates, capacitance between inductor turns and interconnections inductances and capacitances. In these conditions, also electromagnetic radiations occur and all these effects become significant at microwave frequencies.

1-1-2 Concept of distributed parameters:

The previous limitations of the lumped circuits prompted the development of a new approach called the distributed circuit approach. In the thirties, circuits composed of transmission lines in which the electromagnetic fields are bound in the transverse direction came into existence. Among these transmission lines the coaxial line and the rectangular waveguide became the most popular. The emphasis was shifted from the currents flowing inside the conductors to the electromagnetic waves propagating in the space inside these transmission lines. In a coaxial line, the lowest order mode is a transverse electromagnetic (TEM) mode in the case of which the transmission line can be characterized by capacitances and inductances distributed along the length. In the rectangular waveguide, the electromagnetic fields configuration is described in terms of transverse electric (TE) and transverse magnetic (TM) modes and there exits an useful analogy between the fields strength and voltages and currents in suitably loaded transmission lines, thus enabling the guide to be represented as a distributed networtk.

1-1-3 Microwave semiconductor devices:

During the second world war, microwave circuits and technology using coaxial lines and waveguides got a rapid development leading to the emergenge of klystrons, magnetrons, travelling wave tubes, etc ...

In the early 1950's, when the microwave technology, after war time secrecy and military applications, penetrates the civil world, a tremendous revolution was achieved in both techniques

and technologies. The introduction of semiconductor device technology brought solid state devices and led to a rapid progress in microwave technology after 1965. A number of devices were developed to perform various microwave functions such as power generation, mixing, switching, amplification, etc. These include the IMPATT diode, Gunn diode, Schottky barrier diode, PIN diode, Gallium Arsenide field effect transistor and Silicium bipolar transistor. Small size semiconductor devices were available and it was necessary to find transmission media compatible with these devices.

1-1-4 Microwave transmission lines:

The solution was the use of planar transmission lines whose first kind, called "strip transmission line or stripline", was proposed by Barret and Barnes in early 1951. The structure is mainly a strip conductor sandwitched between two dielectric substrates with conductive plating on the two outer sides , Fig.1-1a. In 1952, another basic transmission line called "microstrip line" was conceived. It consists of a dielectric substrate with a strip conductor on one side and a conducting plane on the other side, Fig.1-1b. Unlike the stipline, the microstrip is basically an open structure and requires a high dielectric constant substrate to confine the electromagnetic fields near the strip conductor. In the 1950's, these transmission lines were analyzed by studying their impedance, radiation, discontinuity effects, etc. However, microwave components using these elements did not become popular because low loss dielectric materials with reproducible characteristics, at microwave frequencies were not available.

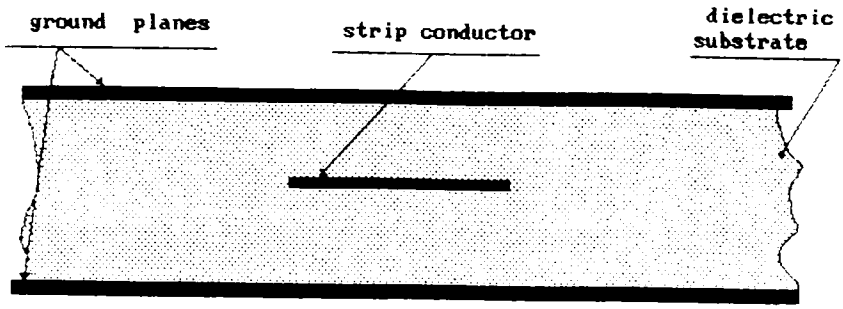

(a) Stripline (TEM mode).

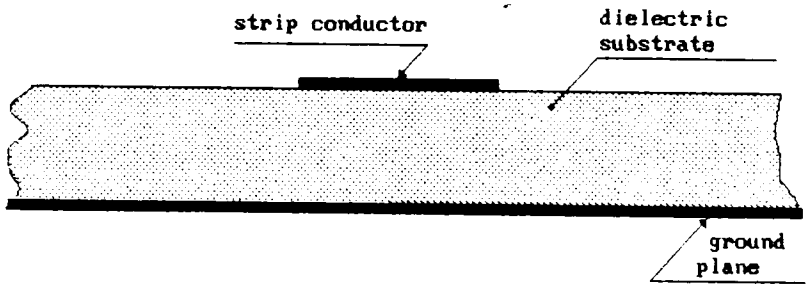

(b) Microstrip line (quasi-TEM mode).

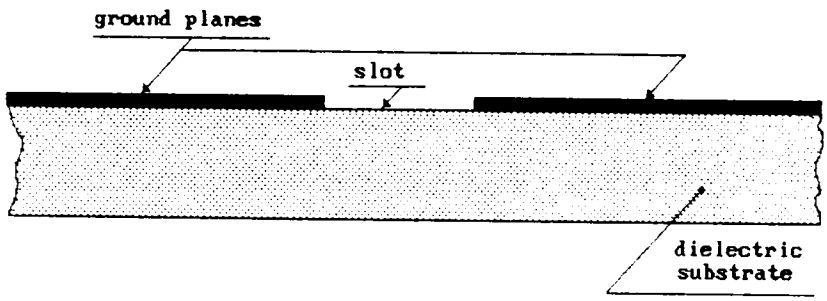

(c) Slotline (non TEM mode).

Fig.1-1. Cross-sectional views of the basic transmission lines.

1-1-5 Microwave integrated circuits:

During the 1960's, with progress in materials technology and fabrication processes, namely the deposition of metallic films using the thin and thick film technologies, the interest in planar transmission lines was revived. The integration of planar transmission lines resulted in the beginning of the evolution of a new circuit form called Microwave Integrated Circuits (MIC's) in the late 1960s. In 1968, a third type of planar transmission line named the "slot line" was proposed by Cohn. This structure consists of a slot etched from the conducting layer on one side of the dielectric substrate, the other side being bare, Fig.1-1c. Subsequent, various other planar transmission lines, which form variants of the stripline, microstrip line and slot line were evolved ever widening the scope of applicability of MICs. Among them, the suspended stripline, suspended microstrip, inverted microstrip, coplanar waveguide and coplanar strips.

1-1-6 Hybrid technology:

Development in vacuum deposition techniques and photolithography allowed the realisation of lumped circuit elements such as the single turn inductor, spiral inductor, interdigitated capacitors and resistors. The process of fabricating MICs by soldering or bounding semiconductors devices on the passive circuit composed of planar transmission lines and lumped elements, has been termed "hybrid technology" and the circuits realized are called "hybrid MICs".
Since 1970, an important progress in hybrid MICs has led to compact integrated modules with highly reliable performance.

Presently, the monolithic technology permits the insertion of the active devices in a semiconducting substrate that contains passive elements and interconnections, resulting in a much higher degree of miniaturisation and integration. The materials used are namely Silicon (Si) and particularly Gallium Arsenide suitable for building Monolithic Microwave Integrated Circuits (MMICs).

1-1-7 Monolithic microwave integrated circuits:

The last two decades have been a revolution in techniques and technologies of microwave systems through the use of MIC's in microwave radars, communications, navigation and sensing systems. With the emerging GaAs technology, MMIC's are receiving increasing attention for the next generation of microwave components. The monolithic approach offers promising future for millimeter-wave IC's and for systems desiring extremely wide band capabilities.

1-2 MIC's interconnections:

1-2-1 The main interconnections:

In both hybrid and monolithic microwave integrated circuits, planar transmission lines are the basic interconnection media. There are three main versions of the planar transmission lines - the stripline, the microstripline and the slot line (Fig.1-1).
There are other variants of these lines - suspended lines, suspended microstrip, inverted microstrip, coplanar waveguide and coplanar strips (Fig.1-2).

1-2-2 Propagation modes in the interconnections:

In a stripline, the dominant mode of propagation is the transverse electromagnetic (TEM); while in a microstripline, as the medium is inhomogeneous, the TEM mode can not exist. However, at low microwave frequencies, the propagation is close to TEM; the longitudinal magnetic and electric fields are negligible compared to the transverse fields and the mode is said "Quasi-TEM". In a slotline, the dominant mode is essentially non TEM.

1-2-3 Microstrip interconnections:

Regarding the wide applications of microstrip lines in MIC's, we will focus on these transmission lines. They are very useful for the microwave and millimeter-wave hybrid and monolithic integrated circuits required for solid state systems because of their simplicity and planar structure. A planar configuration implies that the characteristics of the circuit element can be determined by the dimensions in a single plane.

Transmission lines and passive lumped or distributed circuit elements, which are manufactured and assembled from planar metal conductors or conducting strips on insulating substrates, are essential basic elements in MIC's and MMIC's. The metal strips or microstrips are deposited by thin film or thick film technology on dielectric substrates. The processing steps are substantially different compared to conventional coaxial and waveguide circuit technology.

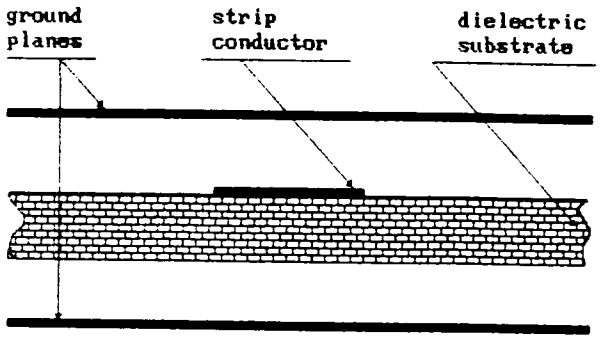

(a) Suspended stripline.

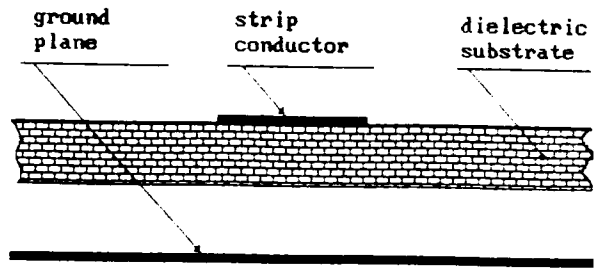

(b) Suspended microstrip.

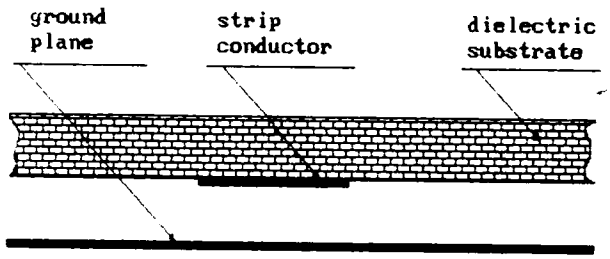

(c) Inverted microstrip.

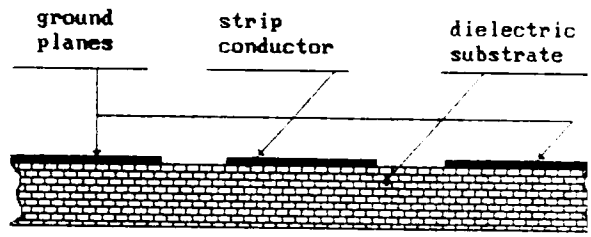

(d) Coplanar waveguide.

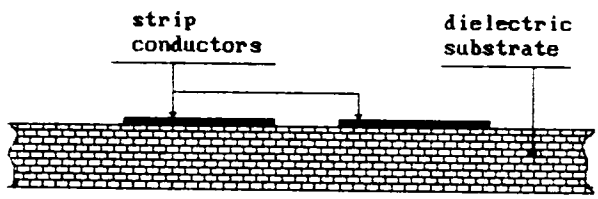

(e) Coplanar strips.

Fig.1-2. Cross-sectional views of some variants of the basic microwave transmission lines.

1-2-4 The microstrip transmission lines advantages:

Circuit built with microstrip transmission lines or microstrip components have three important advantages:

- The complete conductor pattern can be deposited and processed on a single dielectric substrate which is supported by a single metal ground plane. Such a circuit can be fabricated at a substantially lower cost than waveguide or coaxial circuit configurations.
- Active and passive devices can be bonded directly to metal strips on the dielectric substrate.
- Devices and components incorporated into IC's are accessible for probing and circuit measurements (with some limitations imposed by external shielding requirements).

Although the microstrip has a very simple geometric structure, the electromagnetic fields involved are actually complex. Accurate and thorough analyses require quite elaborate mathematical treatment.

1-3 MIC discontinuities:

Microwave integrated circuits based on microstrip transmission lines involve necessarly discontinuities in the strip conductors . These discontinuities result from abrupt changes in the geometry of the strip conductor. Their characterization is therefore essential for accurate design of MIC's as well as the capacitance calculations of arbitrary shaped conductors located on parallel planes.

1-3-1 The general discontinuities.

The discontinuities generally encountered in practice are of the following types:

-Abruptly ended strip conductor.

-Rectangular conductor patch.

-Series gap in the strip conductor.

-Step change in width.

-Right angle bend.

-Bends of arbitrary angle.

-Tee junction.

-Cross junction.

-Slot in the strip conductor.

(see Fig.1-3.)

1-3-2 Discontinuities modelization.

In general the dimensions of the discontinuities are much smaller than the wavelength, and hence, they can be approximated by equivalent circuits consisting of various lumped elements resulting from the accumulated charges at the end regions of the conductors. There will be electric currents flowing in the end region, corresponding to the extra charges, and there will be a measurable amount of radiated energy loss. Consequentially, the discontinuity physically realized, in fact, has the network appearance of an RLC network:
a resistive component to account for the radiated energy, an inductive component to represent the extra currents and a capacitive component corresponding to the extra charges on the discontinuity end corners **[1]**,**[2]**, and **[12]**.

(a) Abruptly ended strip conductor.

(b) Rectangular conductor patch. (resonator)

(c) Series gap in the strip conductor.

(d) Step change in width.

(e) Right angle bend.

(f) Bend of arbitrary angle.

(g) Tee junction.

(h) Cross junction.

(i) Transverse slit in the strip conductor.

Fig.1-3. Top views of the generally encountered microstrip discontinuities.

In practical work, for the frequency range up to 1 GHz, the electromagnetic energy lost by radiation and through inductive components is negligible according to published experiments. At frequencies in the range 1- 20 GHz, the radiation and the currents redistribution at the conductor corners become measurable and significant. However, the capacitance aspect is the dominant part for many discontinuities such as open-end, square and rectangular microstrips.

1-4 Mathematical methods for microstrip analysis:

The various methods of microstrip analysis may be divided into three groups [2].

The first group comprises quasi-static methods as the modified conformal transformation method, finite difference method (FDM), integral equation techniques and variational method in Fourier transformed domain. In this approximation, the nature of wave propagation is considered to be pure TEM and microstrip characteristics are calculated from the electrostatic capacitances as will be detailed further (section 1-5). It is found that this analysis is adequate for designing circuits at the lower microwave frequencies (below X-band) where the strip width and the substrate thickness are much more smaller than the wavelength in the dielectric material.

In the second group, called the dispersion models, the deviation from the TEM nature is accounted for quasi-empirically. Some parameters of the model are determined such that the final expression agrees with the known experimental (or exact theoretical) dispersion behaviour of the microstrip. This group comprises: coupled TEM and TM modes

models, ridged waveguide model, planar waveguide model and coupled TEM/TE-lines models.

The third group, in which the full-wave analysis is accomplished by considering the hybrid nature of the mode of propagation, includes: integral equation method, Galerkin's method in FTD for open microstrips. For enclosed microstrips: finite difference method, integral equation methods and Galerkin's method in FTD.

1-5 Microstrip quasi-TEM analysis:

When at least two conductors are located in a homogeneous dielectric medium, the TEM analysis is applied. In the case of a microstrip, the two conductors, i.e, the strip and the ground plane are no more in a homogeneous medium as shown in Fig.1-1. Gupta et al.[2] have used Maxwell's equations to convincingly demonstrate the necessity for longitudinal components of electric and magnetic fields. This is clearly inconsistent with a pure TEM propagating mode. However, at lower microwave frequencies (below X-band), where the strip width and the substrate thickness are much smaller than the wavelength in the dielectric material, the propagation can be considered TEM with a good accuracy. In this frequency range, the longitudinal magnetic and electric fields components are neglected compared to the transversal fields and the quasi-static analysis yields to good results.

In this approach, the microstrip transmission characteristics are calculated from the values of two electrostatic capacitances Ca and C [2]:
First, Ca is determined for a unit length of the microstrip with the dielectric substrate replaced by air.

Second, C is calculated for a unit length of the microstrip with the dielectric substrate present.

Then, values of characteristic impedance Z_0, phase constant β and the effective permitivity ϵ_{eff} can be written in terms of these capacitances as follows :

$$Z_0 = \frac{1}{c\sqrt{CCa}} \qquad (1-1)$$

$$\beta = \beta_0 \sqrt{\frac{C}{Ca}} \qquad (1-2)$$

$$\epsilon_{eff} = \frac{C}{Ca} \qquad (1-3)$$

$$\beta_0 = \frac{w}{c} \qquad (1-4)$$

where c is the velocity of the electromagnetic waves in free space. ϵ_{eff} is the effective dielectric permitivity that takes into account the fields in the air region, β_0 is the phase constant in free space and w is the wave radial frequency.

The electrostatic capacitances per unit length Ca and C can be calculated by relating the strip electric potential to its charge density in the transversal plane (perpendicular to the propagation axis). The electric potential is evaluated in each dielectric medium by solving Laplace's equation, which is deduced from Maxwell's equations (see Appendix A). Then, applying the continuity conditions to the air-dielectric substrate interface containing the conductor, an expression relating the strip charge density to its electric potential is determined leading to the electrostatic capacitance per unit length.

1-6 Mathematical methods applied to quasi-TEM approach:

There are many methods used in quasi-static approach for the calculation of the electrostatic capacitance [2], [17 to 27]. They can be classified in two groups: the first including methods dealing with two dimensional problems and the second containing techniques for three-dimensional problems. For constant cross-section or infinitely long microstrip structures, the calculation of propagation parameters reduces essentially to the solution of a two dimensional Laplace's equation subject to boundary conditions determined by the structure geometry. There are many methods which exist to solve this problem. The commonly reported ones are the conformal transformation method, the finite difference method, the integral equation technique and the variational method in Fourier Transformed Domain (FTD).

1-6-1 Constant cross-section structures:

1-6-1-1 Conformal transformation method:

This method, introduced by Wheeler [5], is based on transformations from the microstrip plane to a parallel plate capacitor plane where the dielectric substrate cross-section is no more homogeneous but partially filled with air. The transformation functions depend on the strip width to dielectric substrate ratio and lead to closed formulas for the microstrip impedance [17].

The method is exact and has been applied to obtain closed form expressions for the characteristic impedance of the homogeneous stripline. However for structures with

inhomogeneous medium, the application of this method becomes prohibitively complicated and the conductor thickness as well as the microstrip enclosure are ignored.

1-6-1-2 The finite difference method:

This method is based on the numerical solution of Laplace's equation in finite difference form **[17],[21] and [27]**. It is suitable for enclosed microstrip and the conductor thickness can easily be incorporated into the analysis. In this method, the electric potential is considered at grid points where it is expressed in terms of the potentials of the four points that are in the immediate vicinity. A " relaxation method " is used to determine the grid points potentials with an allowed error. The charge on the strip is calculated by integrating the potential over the conductor surface and finally, the capacitance is determined as the charge to potential ratio.

1-6-1-3 The integral equation method:

In this method, the microstrip analysis is formulated in the form of integral equation rather than differential equation **[17], [18]**. This analysis is divided into two points. First, the formulation of a suitable Green's function and second, the solution of an integral equation expressing the electric potential in terms of the Green's function and the charge distribution. The solution is obtained by writing the integral equation in matrix form where the potential vector is related to the charge vector by a matrix which, when inverted, leads

to the conductor capacitance. Green's function for the microstrip configuration is obtained from the theory of images.

1-6-1-4 The variational method in Fourier Transformed Domain (FTD):

The search of microstrip analysis techniques which are computationally more efficient has led to the "Variational method in FTD" **[6], [17]**. In fact, there are two significant features of this method. First, a variational method of calculating the capacitance from the charge density which avoids the need for knowing the charge distribution accurately. Secondly, the major portion of analysis is carried out in FTD with the result that the integral equation for the potential gets replaced by an ordinary product of charge density and Green's function. Then, using Parseval's formula, the capacitance is expressed with the transformed charge density and potential. This latter is obtained by solving Laplace's equation which becomes ordinary in the transformed domain and the transformed charge density is calculated by using an approximate trial function that maximizes the capacitance.

1-6-2 Arbitrary shaped metalizations:

For the discontinuities, the problems become three-dimensional and the static values of capacitances can be evaluated by finding the excess charge distribution near the discontinuity end corners. The different methods used for the discontinuities capacitance calculations have been treated by

many authors: Farrar and Adams [11], Maeda [36], Itoh et al. [10], Silvester and Benedek [12]. Among these methods : matrix inversion method, variational method and Galerkin's method in the spectral domain.

1-6-2-1 The matrix inversion method:

The matrix inversion method is a very general approach to find the static capacitance of a conductor of any arbitrary shape on the top surface of the dielectric substrate [11]. In this method, the total conductor area is divided into small subsections over which the charge density is assumed uniform. The potential at any subsection due to the other subsections charges is expressed in matrix form with the help of a three-dimensional Green's function that is obtained using the theory image. Finally, the total conductor capacitance is calculated from the matrix relating the strip potentials and charges.

1-6-2-2 The variational method:

The method uses the variational principle for formulating the capacitance problem [17], [36]. The capacitance is expressed with a suitably chosen potential Green's function and the charge distribution that is used as a trial function to maximize this capacitance.

1-6-2-3 The Galerkin's method in FTD.

In this method a two-dimensional Fourier transform is applied to both electric potential and charge density. Then,

Poisson's equation, the boundary and interface conditions are written in spectral domain. The transformed Poisson's equation is written, using Galerkin's method, in matrix form leading to an expression of the conductor capacitance [26].

1-7 The method of lines.

In quasi-static approach, the method of lines (MoL), as called in mathematical literature, is applied to transform Laplace's equation from the partial differential form to an ordinary differential equation by discretizing all the space variables except one which allows an analytical solution [13 to 16]. Then the continuity conditions applied to the interfaces lead to a matrix that relates the conductors electric charges to their potential yielding the capacitance matrix.

1-8 CONCLUSION:

We have overviewed some of the principal MIC components as well as the overall methods employed to analyze them. From comparison, we conclude that the MoL is the simplest in mathematical formulation with no need of Green's function or series expansions. In the next chapter, we will see how suitable this method is for the analysis of multilayer parallel multiconductor microwave structures.

CHAPTER2

THE METHOD OF LINES APPLIED TO ONE-DIMENSIONAL DISCRETIZATION.

2_1 Introduction

The growth of microwave and high speed digital integrated circuits has rised the necessity to analyze the interconnections problems. In both monolithic microwave integrated circuits and microwave integrated circuits, the optimal positioning of the strips on different dielectric interfaces is a key factor in design. A compromise must be found between the IC size and the unwanted coupling between adjacent elements in high density integrated circuits.

A full-wave analysis of complete MIC's will not be possible in the immediate future with acceptable numerical expense. As alternative solutions, quasi-static field theoretical analyses have been used to analyze such integrated circuits. Many numerical and pseudo-numerical techniques, in quasi-static approach, have been used for evaluating the capacitance and inductance matrices of multiconductor systems. Among these methods, as has been presented in the previous chapter, we can enumerate: the integral equation techniques **[18]**, the method of moments **[19]**, **[20]**, the finite difference method **[21]**, **[1]**, The network analog method **[22]**, **[23]**, the conformal mapping technique **[24]**, **[25]**, and the variational method **[6]**, **[26]** and **[27]**.

Recently, Henrich DIESTEL has applied the method of lines (MoL) to analyze, in quasi-static approach, a monolayer

multiconductor system with isotropic homogeneous dielectric substrate and vanishing thickness strips [15].

The Method of Lines is applied in quasi-static approach by considering the electric potential function and solving Laplace's equation after converting it from the partial differential form to an ordinary one. This is obtained by discretizing, with lines parallel to the **y** direction, the independent variable **x** in which conductors discontinuities occur on the dielectric interfaces and keeping continuous the independent variable **y** which contains the homogeneous dielectric substrates.

Dirichlet's conditions hold on lateral electric walls that belong to the shielding, where the electric potential equals zero while the boundary conditions are set on top and bottom perfect conducting planes composing the shielding as well.

The discretization yields to a system of algebraic equations relating the electric potentials and charges that are in vector forms. After some matrices manipulations and diagonalization, to decouple this system of equations, an expression is found for the electric potential vector in each dielectric substrate. Applying the continuity conditions to the interfaces containing the conductors, the potential vectors are related to the charge density vectors, whose elements are charge densities between consecutive lines, by a real and symmetric matrix. The capacitance is defined only for conductors; then this matrix is reduced to the non-zero charge density elements of the strips and inverted to obtain a microcapacitance matrix relating the "sub-charge densities" of the strips to the "sub-potentials". Finally, the macrocapacitance between conductors is formed by assembling and summing up the microcapacitance elements according to the

strip to which they belong.

This chapter deals with the MoL in quasi-static approach, applied to constant cross-section structures that is with one dimensional discretization. In section two, the history of the MoL is given with the method introduction in the MIC's field. In section three, the method using sinusoidal discretization is clarified by a detailed analysis of a multilayer multiconductor structure followed by an illustrative example and the description of the developed software program.

2-2 The Method of Lines.

The Method of Lines was developed by mathematicians in order to solve partial differential equations [28]. This method has certain similarities with the finite difference method (FDM) from which it differs in the fact that for a given system of partial differential equations, all but one of the independent variables are discretized to obtain a system of ordinary differential equations. This semi-analytical procedure allows an analytical solution and, by this, saves a lot of computing time. The MoL has been applied to various problems in theoretical physics [28]. The advantages of this method are easy formulation, simple convergence behaviour, suitability for comlexe structures, no spurious solution and no need of prior knowledge about the potential function. Also, there is no need to specify specially suited expansion or Green's functions; which is particularly advantageous to the analysis of complex microwave structures. With conventional FDM, large systems of equations are solved while with this pseudo-analytical method the system of equations is reduced considerably.

This method has been first used in 1980 by R. PREGLA and U. SHULZ [13] for the calculation of planar microwave structures which are generally composed of one or more dielectric substrates containing conductors at the interfaces. Regarding the discontinuities due to the conductors, one space independent variable is discretized for constant cross-section structures while two space variables are discretized for the other arbitrary shaped planar microwave structures. The third space variable perpendicular to the interfaces planes is kept continuous as the dielectric substrates are homogeneous. Dirichlet's and/or Neumann's conditions hold on electric and/or magnetic walls disposed perpendicularly to the discretized variable direction while boundary conditions hold on both top and bottom perfectly conducting planes.

The MoL has no relative convergence problem caused by the singular behaviour of the fields at the conductors edges and affecting the techniques where series expansions are truncated. In this method all functions are expanded corresponding to the number of lines and hence with the same accuracy. As a consequence the results always converge correctly ; however the rate of convergence depends on the positioning of the conductors edges between the discretization lines [29], [30].

2-3 The Method of Lines for quasi-static case.

2-3-1 Lateral boundary conditions:

In quasi-static approach, the partial differential equation (Laplace's equation) is solved for the electric potential $\phi_{(x,y)}$. In order to have a unique solution, Dirichlet and/or

Neumann conditions must hold on electric and/or magnetic walls that are normal to the independent space variables.

With the MoL, the Dirichlet's condition ($\phi(x,y)=0$) is realized by positioning the electric wall on a discretization potential line, while the Neumann's condition ($\frac{\partial\phi(x,y)}{\partial x}=0$) is obtained by locating a magnetic wall between two discretization lines having the same electric potential, as may be allowed for symmetric structures (Fig. 2-1).

The four possible left-right boundary conditions are:

DIRICHLET --- DIRICHLET

DIRICHLET --- NEUMANN

NEUMANN --- DIRICHLET

NEUMANN --- NEUMANN

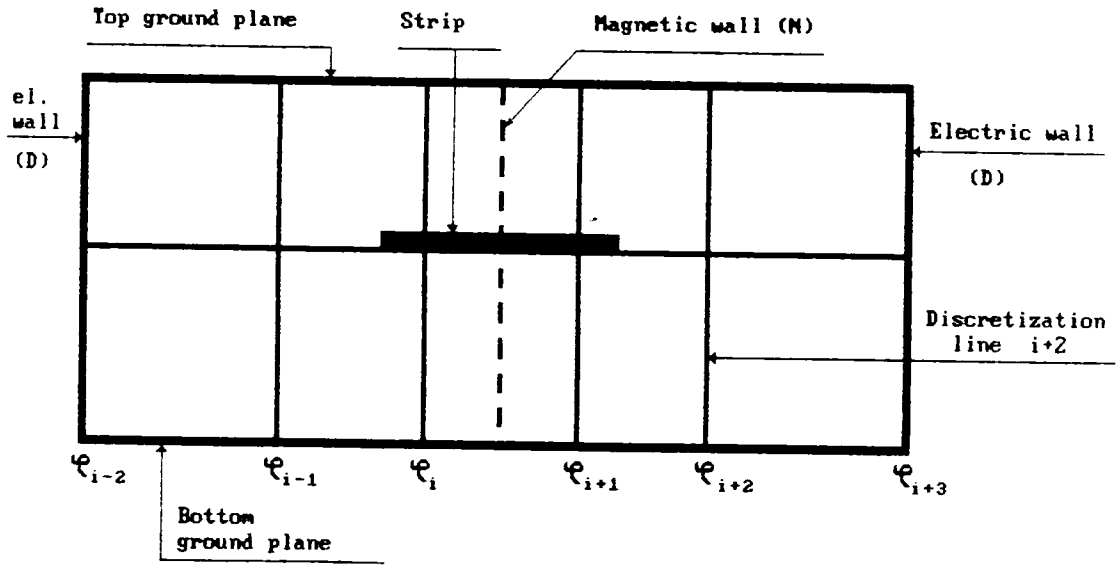

Fig.2-1. Illustration of Dirichlet's and Neumann's conditions.
(D) : Dirichlet.
(N) : Neumann.

2-3-2 Analysis of a multilayer multistrip structure:

Consider the structure shown in Fig.2-2 in which five dielectric layers having permitivities constants ($\epsilon_1, \epsilon_2, \ldots, \epsilon_5$) are bounded by perfectly conducting planes. At the dielectric interfaces 1 and 3, N lossless, zero thickness and infinitely long conductors are located. In the quasi-static analysis the electric potential function $\phi(x,y)$ for each region (I,II,...,V) has to satisfy the partial differential equation:

$$\frac{\partial^2\phi(x,y)}{\partial y^2}+\frac{\partial^2\phi(x,y)}{\partial x^2}=0 \qquad (2-1)$$

and the boundary condition:

$$\phi(x,y)=0 \qquad (2-2)$$

on the electric walls. The continuity conditions have to be considered at the dielectric interfaces while the Dirichlet's conditions hold on the lateral electric walls which are parts of the shielding.

2-3-2-1 Transformation of Laplace's equation:

This boundary value problem is solved elegantly with the MoL in which the electric potential function is discretized in the direction where singularities occur (**x** coordinate) and is expressed analytically on lines where the potential varies smoothly (y coordinate). In Fig.2-2, an arbitrary arrangement of lines is depicted (Fig.2-3). The first derivatives with respect to **x** are evaluated between the

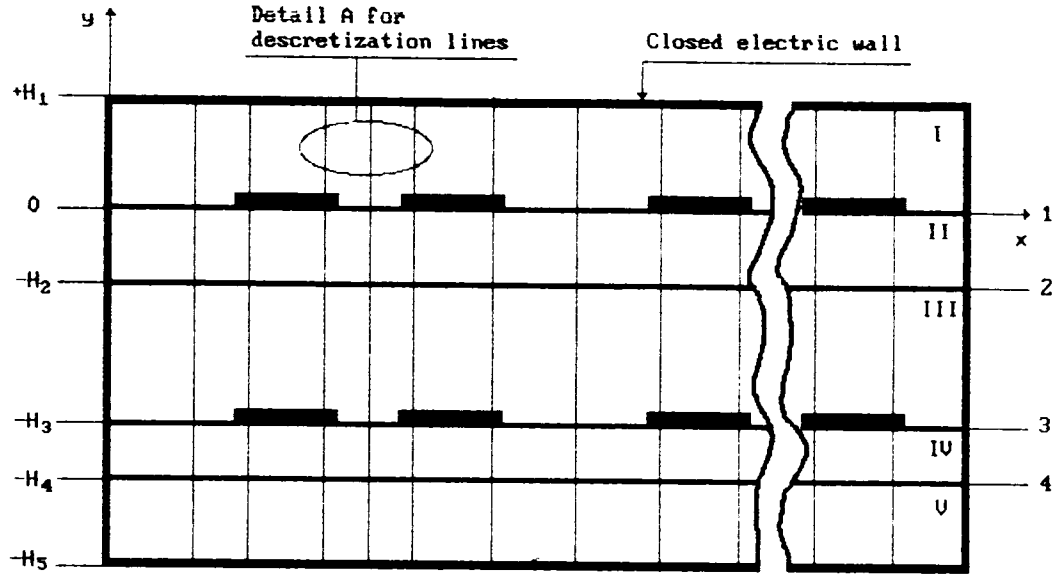

Fig.2-2. Cross-sectional view of a multiconductor multilayer microwave planar structure.

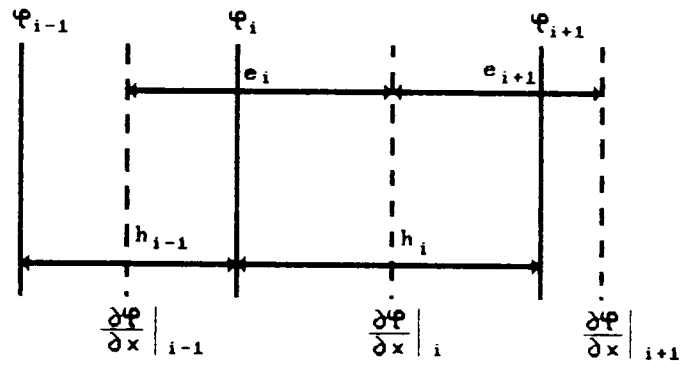

Fig.2-3. Detail A from Fig.2-2. above.

(solid) potential lines on dotted lines which for clearness are not shown in Fig.2-2.

With the abbreviation $\phi(x_i, y) = \phi_i(y)$, the i-th finite difference approximation is:

$$\left.\frac{\partial \phi}{\partial x}\right|_i = \frac{\phi_{i+1} - \phi_i}{h_i} \qquad (2-3)$$

where h_i represents the i-th interval size. The evaluation of the second derivatives is performed on the potential lines. The second derivative is given by

$$\left.\frac{\partial^2 \phi}{\partial x^2}\right|_i = \frac{\left.\frac{\partial \phi}{\partial x}\right|_i - \left.\frac{\partial \phi}{\partial x}\right|_{i-1}}{e_i} \qquad (2-4)$$

with the i-th interval size e_i between dotted lines . In order to obtain symmetric operators in case of non-equidistant discretization, eq.(2-3) is normalized as:

$$\sqrt{\frac{h_i}{h}}\left(h \left.\frac{\partial \phi}{\partial x}\right|_i\right) = \sqrt{\frac{h}{h_i}}(-\phi_i + \phi_{i+1}) \qquad (2-5)$$

$$i=0,1,\ldots,M$$

with the boundary conditions according to (2-2) , i.e $\phi_0 = \phi_{M+1} = 0$, eq.(2-5) can be summarized in the following matrix equation:

$$h r_h^{-1} \phi_x = r_h D \phi \qquad (2-6a)$$

where

$$\phi_x = \left(\frac{\partial \phi}{\partial x}\Big|_0, \ldots, \frac{\partial \phi}{\partial x}\Big|_M\right)^t ;$$

$$\phi = (\phi_1, \ldots, \phi_M)^t \qquad (2-6b)$$

and

$$r_h = diag\left(\sqrt{\frac{h}{h_i}}\right) \qquad (2-6c)$$

The bidiagonal matrix D represents the first order difference operator for Dirichlet-Dirichlet condition:

$$D = \begin{bmatrix} 1 & . & . & 0 \\ -1 & 1 & . & . \\ . & . & . & . \\ . & . & . & 1 \\ 0 & . & . & -1 \end{bmatrix} \qquad (2-7)$$

which is an **M+1 x M** matrix.

Analogously to (2-5) the finite difference equation (2-4) is normalized as:

$$\sqrt{\frac{e_i}{h}}\left(h\frac{\partial^2 \phi}{\partial x^2}\Big|_i\right) = \sqrt{\frac{h}{e_i}}\left(\frac{\partial \phi}{\partial x}\Big|_i - \frac{\partial \phi}{\partial x}\Big|_{i-1}\right) \qquad (2-8)$$

i=1,...,M

In matrix form, eq(2-8) becomes:

$$h r_e^{-1} \phi_{xx} = -r_e D^t \phi_x \qquad (2-9a)$$

where

$$\phi_{xx} = \left(\frac{\partial^2 \phi}{\partial x^2}\Big|_1, \ldots, \frac{\partial^2 \phi}{\partial x^2}\Big|_M \right)^t \qquad (2-9b)$$

and

$$r_e = diag\left(\sqrt{\frac{h}{e_i}} \right) \qquad (2-9c)$$

The matrix D^t is the transpose of matrix D.

The first-order operator **Dx** with respect to the coordinate **x** is defined by :

$$D_x = r_h D r_e \qquad (2-10)$$

from (2-6) and (2-9), we obtain the following important relation :

$$h^2 r_e^{-1} \phi_{xx} = h^2 \Phi_{xx} = -D_x^t D_x \Phi = D_{xx} \Phi \qquad (2-11)$$

The vector :

$$\Phi = \left(\frac{\phi_1}{\sqrt{\frac{h}{e_1}}}, \ldots, \frac{\phi_M}{\sqrt{\frac{h}{e_M}}} \right)^t$$

represents the normalized vector potential. As can be seen on Fig.2-2, e_i is that interval size which is intersected by the line for ϕ_i . This geometrical interpretation holds in general: each line (dashed or solid) has its own interval size.

In the special case of equidistant discretization with $e_i = h_i = h$ we have :

$$\Phi = \phi \qquad (2-12)$$

and

$$r_h = r_e = I \qquad (2-13)$$

where I is the identity matrix, the second order operator **Dxx** then changes into the well known finite difference operator.

In the Method of Lines, for constant cross-section structures, the discretization is performed only in one direction (**x** coordinate). With the relation (2-11), Laplace's equation (2-1) then becomes:

$$\frac{\partial^2}{\partial y^2}\Phi + \frac{1}{h^2} D_{xx}\Phi = 0 \qquad (2-14)$$

The operator **Dxx** is a real symmetric tridiagonal matrix meaning that the potentials are coupled . By orthogonal transformation, the system of equations (2-14) is decoupled and **Dxx** is transformed into the diagonal form of the real and distinct eigenvalues :

$$T^t D_{xx} T = \lambda \qquad (2-15a)$$

where

$$\lambda = diag(\lambda_j), j = 1, \ldots, M \qquad (2-15b)$$

.

For the matrix of eigenvectors **T**, the relation $T^t.T = I$ is valid.

An analytical representation of the eigenvalues and eigenvectors is possible only in the case of equidistant

discretization . In the general case of non-uniform discretization, the eigenvalues and eigenvectors are determined numerically. The " Implicit QL - Method", an accurate, fast and stable technique has been proved to be particularly suited for this purpose [31].

The system of coupled differential equations (2-14) can now be transformed into the following system of decoupled ordinary differential equations:

$$\frac{d^2}{dy^2}(T^t\Phi)+\frac{1}{h^2}(T^tD_{xx}T)(T^t\Phi)=0 \qquad (2-16)$$

or

$$\frac{d^2}{dy^2}V+\frac{1}{h^2}\lambda V=0 \qquad (2-17a)$$

where

$$V=T^t\Phi \qquad (2-17b)$$

is the transformed vector of potentials.

With the substitution $\lambda=-X^2$, (2-17a) yields :

$$\frac{d^2}{dy^2}V-\left(\frac{X}{h}\right)^2V=0 \qquad (2-18)$$

The solutions of these one-dimensional differential equations correspond to the transmission line equations. They can be represented in the form:

$$V(y)=C_1\cosh\sigma(y)+C_2\sinh\sigma(y) \qquad (2-19a)$$

with

$$\sigma = \frac{\chi}{h} \qquad (2-19b)$$

where **V**, σ and the constants C_1, C_2 are vectors of dimension **M** (number of discretization lines).

For the structure shown in Fig. 2-2, according to the chosen **y**-axis origin, the electric potential **V(y)** has the following expressions:

In medium I:

$$V_I(y) = B_1 \frac{\sinh\sigma(y - H_1)}{\cosh\sigma H_1} \qquad (2-20a)$$

In medium II:

$$V_{II}(y) = \frac{A_2\cosh\sigma(y + H_2) + B_2\sinh\sigma(y + H_2)}{\cosh\sigma H_2} \qquad (2-20b)$$

In medium III:

$$V_{III}(y) = \frac{A_3\cosh\sigma(y + H_2 + H_3) + B_3\sinh\sigma(y + H_2 + H_3)}{\cosh\sigma H_3} \qquad (2-20c)$$

In medium IV:

$$V_{IV}(y) = \frac{A_4\cosh\sigma(y + H_2 + H_3 + H_4)}{\cosh\sigma H_4} +$$

$$\frac{B_4 \sinh \sigma(y + H_2 + H_3 + H_4)}{\cosh} \sigma H_4 \qquad (2-20d)$$

In medium V:

$$V_V(y) = \frac{B_5 \sinh \sigma(y + H_2 + H_3 + H_4 + H_5)}{\cosh \sigma H_5} \qquad (2-20e)$$

2-3-2-2 Interface continuity conditions:

The continuity conditions for the normal component of the electric displacement vector has to be satisfied at each interface . By using the expressions of the electric potential, the continuity equations lead at each interface **k/k+1**, to :

$$V_k(y) = V_{k+1}(y) \qquad (2-20f)$$

$$\epsilon_k \frac{dV_k(y)}{dy} - \epsilon_{k+1} \frac{dV_{k+1}(y)}{dy} = S_k \qquad (2-20g)$$

Where **k** = I,II,...,V and S_k is the transformed electric charge density at the dielectric interface between medium **k** and **k+1** (see Fig.2-2).

At interface 1, containing the first set of conductors, and corresponding to y=0, we have:

$$-B_1 \tanh \sigma H_1 = A_2 + B_2 \tanh \sigma H_2 \qquad (2-21a)$$

and

$$\epsilon_1 X B_1 - \epsilon_2 X(A_2 \tanh \sigma H_2 + B_2) = S_I h \qquad (2-21b)$$

At interface 2, with no conductors, and corresponding to $y=-H_2$, we have:

$$\frac{A_2}{\cosh \sigma H_2} = A_3 + B_3 \tanh \sigma H_3 \qquad (2-21c)$$

and

$$\frac{\epsilon_2 X B_2}{\cosh \sigma H_2} - \epsilon_3 X(A_3 \tanh \sigma H_3 + B_3) = 0 \qquad (2-21d)$$

At interface 3, containing the second set of strips, and corresponding to $y=-H_2-H_3$, we obtain:

$$\frac{A_3}{\cosh \sigma H_3} = A_4 + B_4 \tanh \sigma H_4 \qquad (2-21e)$$

and

$$\frac{\epsilon_3 X B_3}{\cosh \sigma H_3} - \epsilon_4 X(A_4 \tanh \sigma H_4 + B_4) = S_{III} h \qquad (2-21f)$$

Finally, at interface 4, with no strips and corresponding to $y=-H_2-H_3-H_4$:

$$\frac{A_4}{\cosh \sigma H_4} = B_5 \tanh \sigma H_5 \qquad (2-21g)$$

and

$$\frac{\epsilon_4 X B_4}{\cosh \sigma H_4} - \epsilon_5 X B_5 = 0 \qquad (2-21-h)$$

Where S_I, S_{III} are respectively the transformed electric charge density vectors at interfaces 1 and 3 (Fig.2-2), which is

explained subsequently.

2-3-2-3 Determination of the capacitance matrix :

The system of equations (2-21) is solved for the constants $B_1, A_2, B_2, A_3, B_3, A_4, B_4$, and B_5 in terms of S_I and S_{III} on each discretization line.

Equations (2-20a)-(2-20c) lead to the potential vectors V_I, V_{III} in terms of the charge density vectors S_I and S_{III}.

At the interfaces 1 and 3, the relation between the transformed potentials and the charge densities is given in matrix form as:

$$\begin{bmatrix} V_I \\ V_{III} \end{bmatrix} = \begin{bmatrix} \Gamma_{11} & \Gamma_{12} \\ \Gamma_{21} & \Gamma_{22} \end{bmatrix} \begin{bmatrix} hS_I \\ hS_{III} \end{bmatrix} \qquad (2-22a)$$

Where the block matrices Γ_{mn} are of order **M x M** .

Equation (2-22a) may be written in the form :

$$V = \Gamma' hS \qquad (2-22b)$$

with

$$V = \begin{bmatrix} V_I \\ V_{III} \end{bmatrix} \qquad (2-22c)$$

and

$$S = \begin{bmatrix} S_I \\ S_{III} \end{bmatrix} \qquad (2-22d)$$

On the conducting strips, a charge q_i is located between two consecutive lines distant of e_i, hence, as the structure has a constant cross-section, the surface charge density that belongs to the i-th line is given by σ_i which is related to the charge q_i by :

$$\sigma_i = \frac{q_i}{e_i} \qquad (2-23)$$

Outside the strip σ_i equals to zero .
In matrix notation we have :

$$\sigma = \frac{1}{h} r_e^2 q \qquad (2-24)$$

The normalized form of eq.(2-24) can be given as :

$$\Sigma = r_e^{-1}\sigma = \frac{1}{h} r_e q = \frac{1}{h} Q = T S \qquad (2-25a)$$

Where the transformed charge density $S = T^t \Sigma$.
Equation (2-22 b) is valid in the transformed domain. With (2-25a), 2-17b) one obtains :

$$\Phi = T \Gamma' T^t Q \qquad (2-25b)$$

or

$$\Phi = \Gamma Q \qquad (2-26)$$

The capital letters, in (2-26), refer to the normalized electric potential and charge vectors and matrices. In the

original domain, (2-26) becomes:

$$\phi = \gamma q \qquad (2-27a)$$

where

$$\gamma_{ik} = \sqrt{\frac{h}{e_i}}\Gamma_{ik}\sqrt{\frac{h}{e_k}} \qquad (2-27b)$$

The structure of the matrix equation (2-27a) can be represented graphically as shown in Fig.2-4; where the hatched areas correspond to the strip regions on which the potential function is constant and the charge is not zero.
The hatched areas are joined together and result in the "reduced matrix" γ_{red} so that from (2-27a), the following matrix equation can be derived :

$$\phi_{red} = \gamma_{red} q_{red} \qquad (2-28)$$

The matrix γ_{red} is real, symmetric and positive definite. Therefore the method of inversion due to Cholesky is particularly suited to obtain the matrix γ_{red}^{-1} [32].
The capacitance matrix can now be derived from γ_{red}^{-1} by summing up the submatrices elements (hatched areas on Fig.2-4), (see appendixB); and one obtains:

$$q = Cu \qquad (2-29)$$

Where $q = (q_1,\ldots,q_{2N})^t$ are the charges per unit length on the strips with the corresponding potentials $u = (\phi_1,\ldots,\phi_{2N})^t$.

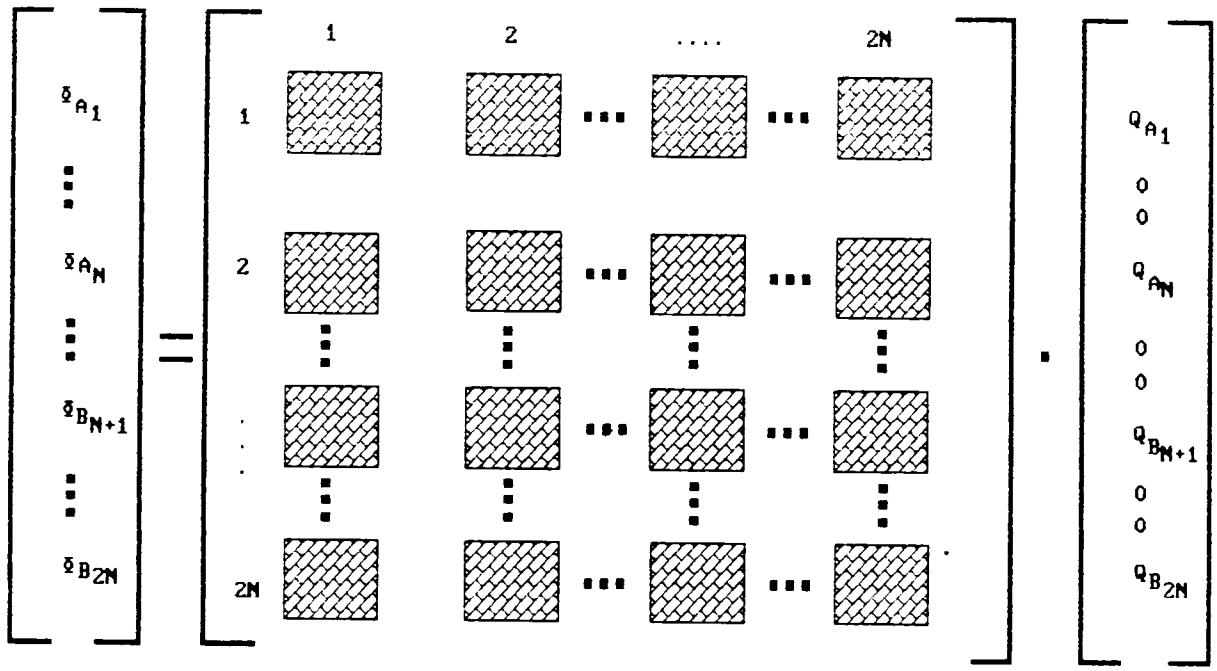

Fig.2-4. Graphical representation of the matrix relating the potential vectors to the charge vectors. The hatched areas represent the submatrices corresponding to the non-zero conductors charges.

2-3-3 Non-equidistant discretization:

The Method of Lines is applied with non-equidistant discretization such that the lines are more concentrated around the conductor edges where fields singularities occur and are more spaced in regions having smoother variations of the fields [15].

In general, the potential function and the surface charge density are unknown. In the present problem, an approximate function for the surface charge density on the conductor is given by the Maxwell distribution which holds exactly only for an isolated conducting strip [33].

If the potential lines are spaced sinusoidally on the strip at

$$x_i = \sin\left(\frac{2i - Mn}{2Mn}\pi\right) \qquad (2-30)$$

Where **Mn** is the total number of lines for the strip **n** and $-1 \le x \le 1$, the same amount of charge is located between any two consecutive lines :

$$\frac{1}{\pi}\int_{x_{i-1}}^{x_i} \frac{dx}{\sqrt{1-x^2}} = \frac{1}{Mn} \qquad (2-31)$$

Because of the singular behaviour of the charge density at the edges, more lines are located near the ends of the strips. The general form of the charge density on the strips between

conducting planes and different dielectrics is similar to that of an isolated conductor. Therefore eq.(2-30) shall be adopted for the present problem and one obtains for a strip, $x_a \le x \le x_b$:

$$x_i = \frac{x_b + x_a}{2} + \frac{x_b - x_a}{2} \sin\left(\frac{2i - Mn}{2Mn}\pi\right) \qquad (2-32)$$

for

$$i = 0, \ldots, Mn$$

At the edge of perfect conducting strips, the field strength is also singular so that eq.(2-32) shall be valid for the regions between edges of different strips. By this, the smallest interval size , located near each edge, can be chosen the same for all these regions so that in the vicinity of every edge the interval sizes are small and nearly symmetric. With the smallest interval $\Delta = x_{Mmin} - x_{Mmin-1}$, where **Mmin** is the number of lines for the smallest strip width or region between strips; the number of lines for each region can be derived from eq.(2-32), so that for $x_a \le x \le x_b$, we have the integer :

$$Mn = \mathrm{INT}\left(\frac{2\pi}{\pi - 2\arcsin[1 - 2\Delta/(x_b - x_a)]}\right) \qquad (2-33)$$

The interval sizes

$$h_i = x_{i+1} - x_i \qquad (2-34)$$

are calculated in a following step from eq.(2-32). While the centers of intervals are deduced from (2-34) as:

$$e_i = \frac{h_{i-1} + h_i}{2} \qquad (2-35)$$

The outer regions which are limited by the lateral walls can be treated in the same way if the intervals are calculated for twice the regions. The intervals have their maximum value near the electric walls where the fields are almost zero. An important advantage of the non-uniform discretization can be recognized in the fact that if the walls are only auxillary quantities, they can be shifted sufficiently far away from the conducting strips without large numerical effort.

At the strips edges, the fields are singular giving rise to problems of convergence for analytical techniques where series expansions are truncated. In the method of lines, all functions are expanded corresponding to the number of lines and hence, with the same accuracy. As a consequence, the result always converges correctly. However, the rate of convergence depends on an edge condition from [29], who considered equal interval sizes and showed that the strip edge should be positioned as illustrated in Fig.2-5.

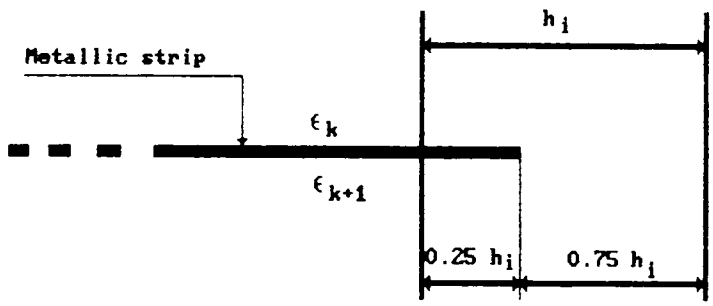

Fig.2-5. Positioning of a strip edge between two discretization lines.

This result is applied to non-uniform discretization as the interval sizes are almost equal near the strip edges. The location of the lines in the regions of strips and spaces is defined by eqs.(2-32) and (2-33). In order to include the edge condition, the interval sizes on the strips have to be shortened by the factor :

$$F = \frac{W - \frac{2\Delta}{3}}{W} \qquad (2-36)$$

which is deduced from the edge conditions [15], with $W = x_b - x_a$, and in a subsequent step the outer interval sizes of the regions between the strips are fitted.

2-3-4 : Illustration for a shielded microstrip line.

Let's consider the simplest microwave structure which consists of a shielded microstrip line as shown in Fig.2-6.

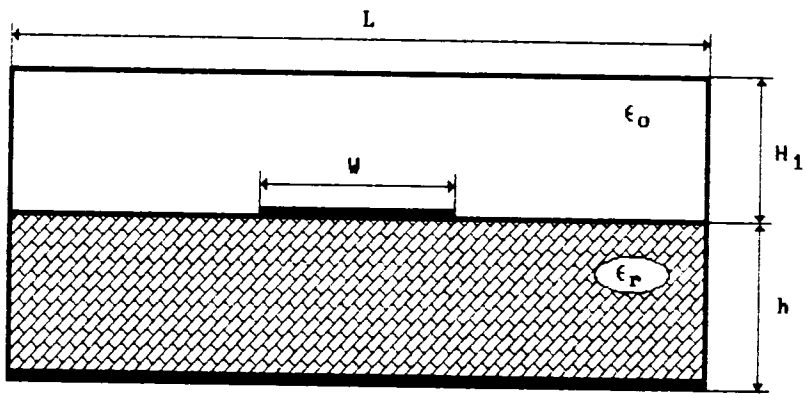

Fig.2-6. Cross-section of a shielded microstrip structure.

Applying eq.(2-32) to $L_{new}-2\Delta$, with **i** varying from $\frac{MS1_{new}}{2}$ to $MS1_{new}-1$, we obtain the **hi** intervals on the left size space region. The next interval which contains the strip edge is equal to Δ.

Equation (2-32) applied to the strip ($x_b-x_a=W-\frac{2\Delta}{3}$), ($\frac{2\Delta}{3}$ to account for edge conditions), **i** varying from 0 to 1, in our case, gives the intervals on the strips. The next interval is equal to Δ.

Equation (2-32) applied to $L_{new}-2\Delta$, with **i** varying from 0 to $\frac{MS1_{new}}{2}-1$, gives the intervals on the right side region.

The discretization leads to the matrices: r_h, r_e, D, D_{xx}.

2-3-4-2 Matrices formation :

The matrix r_h from (2-6 c) has as diagonal elements :

(0.669 , 1.085 , 0.790 , 0.913 , 0.790 , 1.085 , 0.699)

In our case,

$$h=\frac{W}{Mmin+1}=\frac{W}{2}=0.5 \qquad (2-39)$$

From eq. (2-9b), the matrix r_e has as diagonal elements :

(0.831 , 0.904 , 0.845 , 0.845 , 0.904 , 0.831)

From eq.(2-7), as we use Dirichlet's conditions on both

lateral walls, the first order difference operator is :

$$D = \begin{bmatrix} 1 & 0 & 0 & 0 & 0 & 0 \\ -1 & 1 & 0 & 0 & 0 & 0 \\ 0 & -1 & 1 & 0 & 0 & 0 \\ 0 & 0 & -1 & 1 & 0 & 0 \\ 0 & 0 & 0 & -1 & 1 & 0 \\ 0 & 0 & 0 & 0 & -1 & 1 \\ 0 & 0 & 0 & 0 & 0 & -1 \end{bmatrix}$$

From eq. (2-11), the matrix **Dxx** is :

$$Dxx = \begin{bmatrix} -1.150 & 0.885 & 0 & 0 & 0 & 0 \\ 0.885 & -1.473 & 0.477 & 0 & 0 & 0 \\ 0 & 0.477 & -1.042 & 0.595 & 0 & 0 \\ 0 & 0 & 0.595 & -1.042 & 0.477 & 0 \\ 0 & 0 & 0 & 0.477 & -1.473 & 0.885 \\ 0 & 0 & 0 & 0 & 0.885 & -1.150 \end{bmatrix}$$

The diagonal elements of the eigenvalue matrix of **Dxx** are :

(-0.336 , -0.091 , -0.692 , -1.525 , -2.386 , -2.399)

The eigenvector matrix of **Dxx** is :

$$T = \begin{bmatrix} 0.505 & 0.315 & 0.468 & 0.335 & 0.426 & 0.364 \\ 0.465 & 0.377 & 0.242 & -0.142 & -0.546 & -0.514 \\ 0.170 & 0.508 & -0.471 & -0.606 & 0.142 & 0.322 \\ -1.170 & 0.508 & -0.471 & 0.606 & 0.142 & 0.322 \\ 0.465 & 0.377 & 0.242 & 0.142 & -0.546 & 0.514 \\ -0.505 & 0.315 & 0.468 & -0.335 & 0.426 & -0.364 \end{bmatrix}$$

2-3-4-3 Capacitance matrix formation:

Applying the equations (2-19) through (2-25b), we end up with the diagonal matrix Γ' whose elements Γ'_{ii} are given by :

$$\Gamma'(i,i) = \frac{\tanh \sigma_i H_1 \tanh \sigma_i h}{\epsilon_1 X_i} \left(\tanh \sigma_i h + \frac{\epsilon_2}{\epsilon_1} \tanh \sigma_i H_1 \right)$$

(2-40)

The diagonal elements of the matrix Γ' are :

(0.962 , 1.635 , 0.601 , 0.405 , 0.331 , 0.323)

The matrix Γ , in the original domain, from (2-27b), is :

$$\Gamma_{nor} = \begin{bmatrix} 0.457 & 0.232 & 0.126 & 0.084 & 0.048 & 0.032 \\ 0.232 & 0.528 & 0.206 & 0.129 & 0.072 & 0.048 \\ 0.126 & 0.206 & 0.549 & 0.253 & 0.129 & 0.084 \\ 0.084 & 0.129 & 0.253 & 0.549 & 0.206 & 0.126 \\ 0.048 & 0.072 & 0.129 & 0.206 & 0.528 & 0.232 \\ 0.032 & 0.048 & 0.084 & 0.125 & 0.232 & 0.457 \end{bmatrix}$$

In our case, the reduced matrix γ_{red} is :

$$\gamma_{red} = \begin{bmatrix} 0.549 & 0.253 \\ 0.253 & 0.549 \end{bmatrix}$$

The microcapacitance matrix γ_{red}^{-1} is :

$$Cmic = \begin{bmatrix} 2.312 & -1.066 \\ -1.066 & 2.312 \end{bmatrix}$$

The macrocapacitance, in this case a scalar obtained by summing up the elements of matrix **Cmic** as only one conductor is considered, is :

$$\gamma_{red}^{-1} = \frac{Cmac}{\epsilon_o} = 2.492 \text{ pF/m.}$$

2-3-5 Software description

As shown in Fig.2-7, the software program runs as follows:

1-The user of our developed software should first input the geometric and electric characteristics of the structure (strip width **W**, strips number **N**, gap spacing **SS**, structure cross-section width **L**, the smallest number of lines in the smallest region **Mmin**, the dielectrics permitivities and the subtrates thicknesses.).

Then, the software will determine:

2-The smallest interval size using (eq.2-34) with **W** replaced by **SS** if the gap spacing is smaller than the strip width.

3-The scaling factor **h** = (smallest region / (**Mmin+1**)).

4-The positioning of the discretization lines on the total cross-section of the structure from equations (2-32 and 2-33) that are applied to the metalization and gap regions. The Dirichlet-Dirichlet condition is realized by coinciding a line on each lateral electric wall (eq.2-38). The strip edge condition is rspected by positioning the conductor edge at a distance $\frac{\Delta}{3}$ from the left line and at Δ from the right line (eq.2-36) as shown in Fig.2-5.

5-The normalization matrices r_h and r_e given by (2-8c) and (2-9c), by storing the intervals h_i , e_i and the lines number **M** during their evaluations.

6-The second order difference operator **D** and its transpose D^t by (eq.2-7).

7-The matrices D_x,D_x^t and D_{xx} are using (eqs.2-10, 2-11).

8-The eigenvalue and eigenvector matrices λ,T of **Dxx** using the QL algorithm.

9-The matrix Γ, relating the potential and charge vectors at

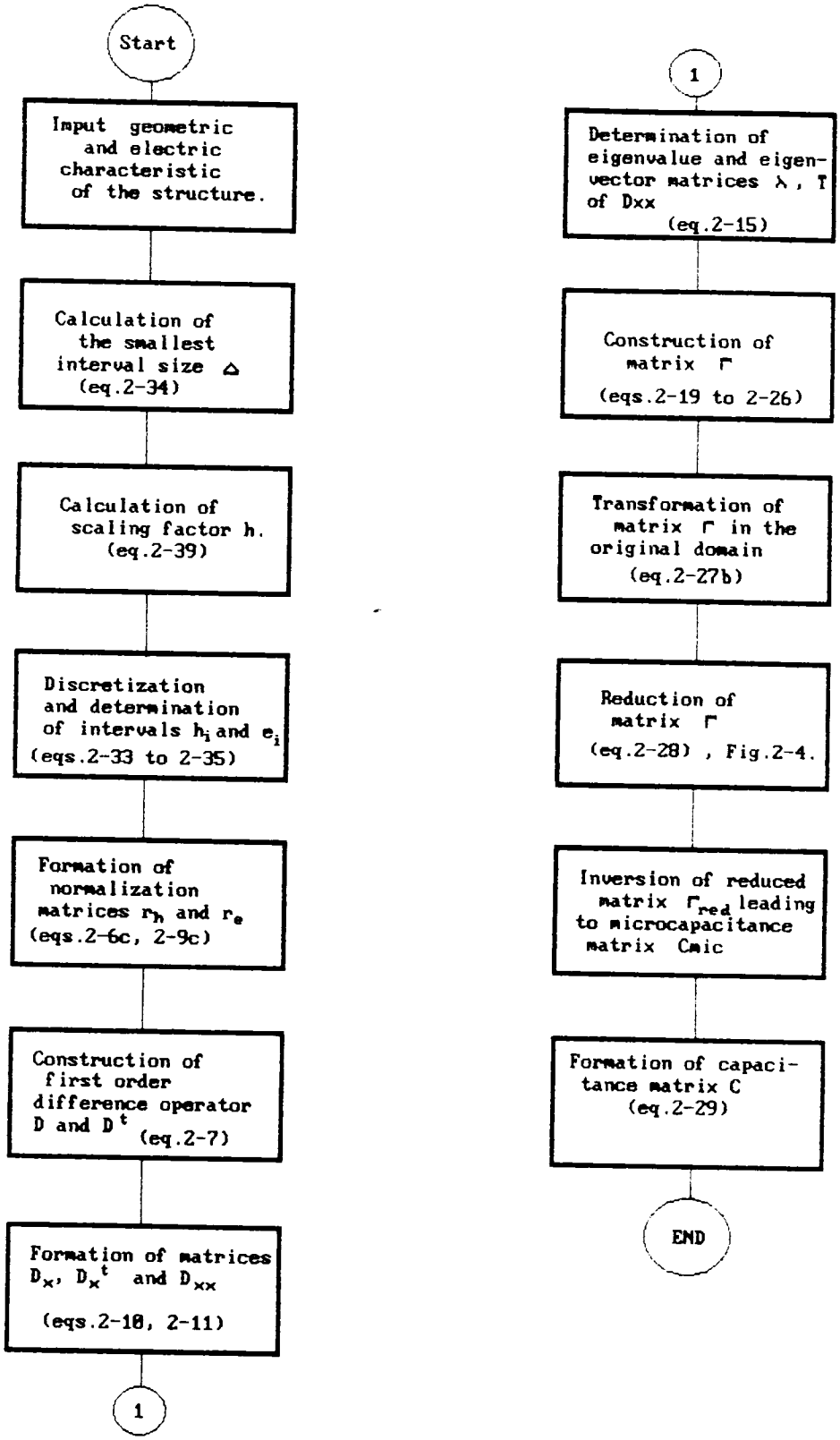

Fig.2-7. Flowchart of the software program using one-dimensional discretization.

the conductor interfaces, by solving the system of equations for each discretization line, (eqs. 2-20 to 2-26).

10-The matrix Γ in the original domain by (eq.2-27b).

11-The matrix Γ in the original domain which is reduced to the non-zero charges of the conductors (Fig.2-4), (eq.2-28).

12-The reduced matrix Y_{red} inverts it and sums it up appropriately to obtain the capacitance matrix.

2-4 Conclusion.

We have shown the application of the MoL to the calculation of the capacitance matrix in the case of two layers of parallel conductors. The extension to more layers of strips can be easily carried on by increasing the system of equations governing the continuity conditions on the dielectric- -substrates interfaces. The structures analyzed in this chapter represent the interconnections joining MIC components which have, generally, arbitrary shapes involving discretization in two space directions. In the next chapter, some of these three-dimensional problems will be analyzed with this method.

CHAPTER3

THE METHOD OF LINES APPLIED TO THREE-DIMENSIONAL PROBLEMS:

3-1 Introduction :

In MIC's and MMIC's, three-dimensional problems are rising due to both isolated crossing interconnections and arbitrary shaped conductors on parallel dielectric substrates. In chapter two, constant cross-sectional structures were considered; however, in practice, digital IC's contain isolated interconnections crossing orthogonally . In MMIC's, these crossings occur as air bridges or underpasses for spiral inductors and directional couplers.

Little has been reported in litterature to analyze such complex structures. A static spectral-domaine approach is used to calculate the coupling capacitances of air bridges and underpasses **[34]**. The generalized "transverse resonance technique" is used in full-wave analysis for circuits parameters determination of a stripline crossing **[35]**; however it is inefficient with crossing multiconductors. But the MoL, with two dimensional discretization, has shown a great suitability to deal with multiconductors crossing orthogonally and to determine their coupling capacitance matrix **[16]**.

The design and packaging of MIC's require also, the calculation of capacitances for arbitrary shaped conductors located on parallel planes. Many papers have been published concerning the capacitance calculation for open circuits,

change of width, gap in microstrip and rectangular section in microstrip. The methods used are various, among them: Galerkin's method in spectral domain **[10]**, Green's function based on variational principle **[36]**, integral equation with computer solution technique **[12]**, and **[37]**.

In this chapter, the MoL, with two dimensional discretization, is applied to three dimensional problems; that is microstrips having discontinuities in two space directions. In section two, this method is used for the calculation of the coupling capacitance of two isolated orthogonally crossing conductors. In section three, the application of this method to the analysis of microstrip sections and discontinuities is deduced from (3-2). In section four, the MoL is extended to anisotropic dielectrics with diagonal tensor permitivities. Finally, in section five, the software program, based on the MoL is described.

3-2 Analysis of two crossing conductors.

3-2-1 Three dimensional Laplace's equation transformation:

We analyze the structure, shown in Fig.3-1, composed of two conductors, crossing orthogonally, of length L_1, L_2 , and widths W_1, W_2, having vanishing thickness and separated by a perfect homogeneous dielectric substrate of thickness **h**.

We consider the potential function $\phi(x,y,z)$ which must satisfy Laplace's differential equation :

$$\frac{\partial^2\phi}{\partial x^2}+\frac{\partial^2\phi}{\partial y^2}+\frac{\partial^2\phi}{\partial z^2}=0 \qquad (3-1)$$

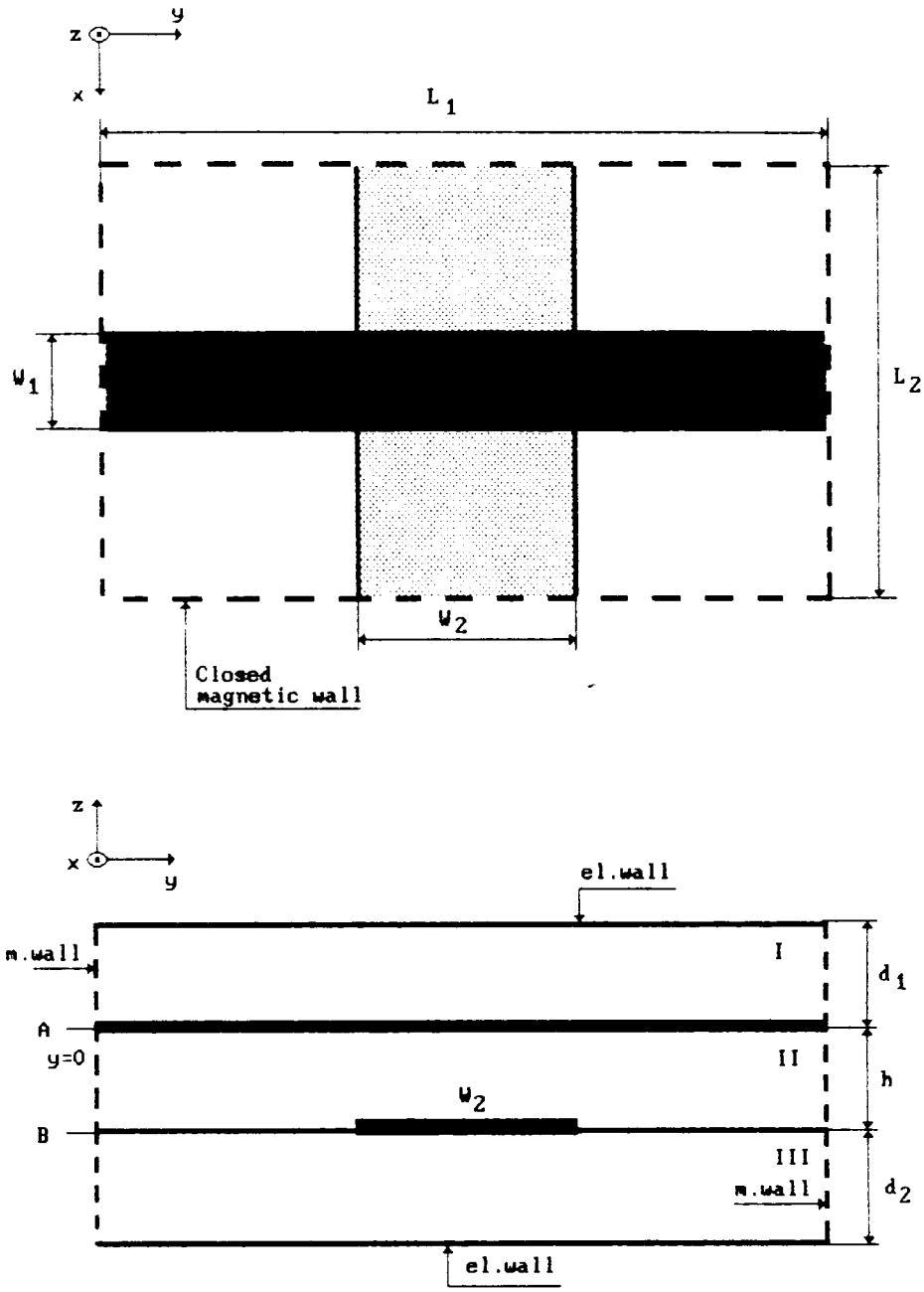

Fif.3-1. Top and cross-sectional views of two orthogonally crossing conductors at different dielectric interfaces.

in the different regions I, II and III (Fig.3-1). Neumann's conditions hold on magnetic walls. To solve this boundary value problem using the MoL, the differential quotients with respect to **x** and **y** , in Laplace's equation (3-1), are approximated by finite difference expressions.

A typical pattern of discretization for two crossing strips, is illustrated in Fig.3-2. The lines of discretization run parallel to the **z** axis and are marked by "+" and "." in the **x-y** plane. The potential function $\phi(x_i, y_k, z)$ noted $\phi_{i,k}$ and the second derivatives $\phi_{xx}(x_i, y_k, z)$ and $\phi_{yy}(x_i, y_k, z)$ are evaluated at the line (x_i, y_k, z) marked "+" in the detail (Fig.3-2). The first derivatives are related to locations between the potential lines i.e. $\phi_x(y_k, z)|_i$ is evaluated at point "**a**" and $\phi_y(x_i, z)|_k$ is determined at location "**b**" (see Fig.3-2). The mixed derivative $\phi_{xy}(z)|_{i,k}$ is calculated at one of the corners of the rectangular mesh of area $e_{x_i} x e_{y_k}$, illustrated by the dots ".".

With the MoL, the potential function is discretized with respect to both **x** and **y**; i.e. the differential quotients for these variables are approximated by finite difference expressions as shown previously eq.(2-3). If we define the first order operator with respect to **x** by

$$[\overline{D_x}] = [r_{hx}][D_x][r_{ex}] \qquad (3-2)$$

Where $[D_x]$ denotes a bidiagonal difference operator for Neumann-Neumann conditions as:

$$[Dx] = \begin{bmatrix} -1 & 1 & . & . & 0 \\ 0 & -1 & 1 & . & 0 \\ . & . & . & . & . \\ 0 & . & . & -1 & 1 \end{bmatrix} \qquad (3-3)$$

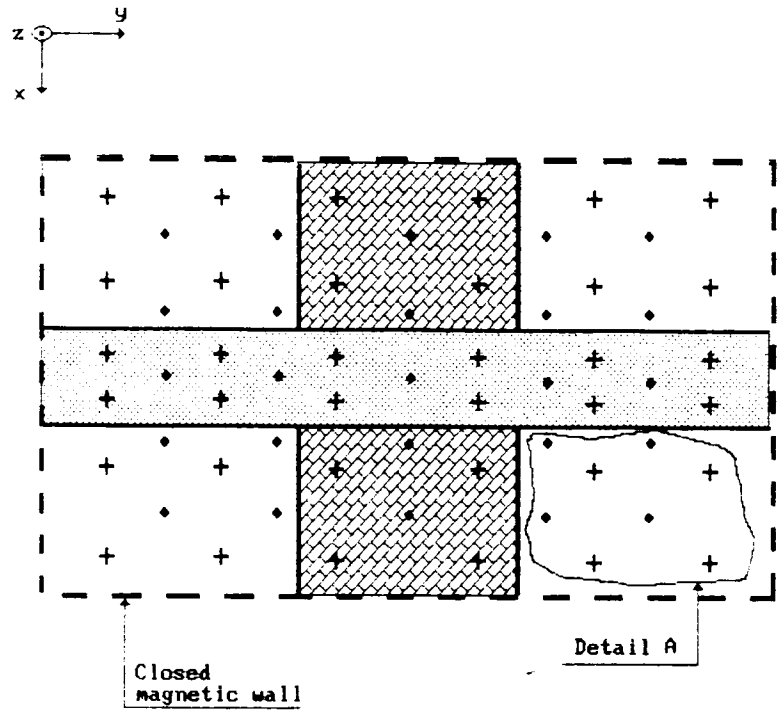

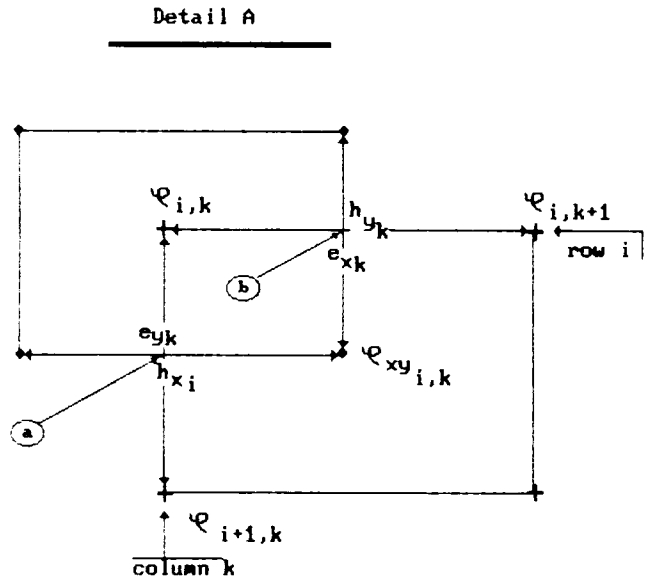

Fig.3-2. Non-equidistant discretization pattern for two crossing conductors. The dots (•) correspond to the mixed dderivatives while the plus (+) represent the potential lines.

the following approximate relation for the matrix of the $M_x x M_y$ second derivatives holds :

$$h^2[r_{ex}]^{-1}[\phi_{xx}][r_{ey}]^{-1} = h^2[\Phi_{xx}]$$

$$= -[\overline{D}_x]^t[\overline{D}_x][\Phi] = -[\overline{D}_{xx}][\Phi] \qquad (3-4)$$

Mx and **My** are respectively the number of discretization lines in **x** and **y** coordinates.

The elements of the matrix [Φ] represent the normalized potentials

$$[\Phi]_{i,k} = \frac{[\phi]_{i,k}}{(\sqrt{\frac{h}{e_{x_i}}}\sqrt{\frac{h}{e_{y_k}}})} \qquad (3-5)$$

The normalization matrices are:

$$[r_{e_x(e_y)}] = diag(\sqrt{\frac{h}{e_{x_i(y_k)}}} \qquad (3-6)$$

and

$$[r_{h_x(h_y)}] = diag(\sqrt{\frac{h}{h_{x_i(y_k)}}}) \qquad (3-7)$$

A finite difference approximation similar to (3-4) can be given for the second derivatives with respect to **y**. However, for the position of $[\phi]_{i,k}$ in the matrix [ϕ] to equal the position of the corresponding marking "+" in the discretization pattern, we must interchange the matrices of potential and operators $[\overline{D_{yy}}]$, (eq.3-8).

Laplace's differential equation is solved at the **Mx.My** nodes "+". For the normalized potential, the following approximate equation holds :

$$\frac{d^2}{dz^2}[\Phi]+\frac{1}{h^2}[\overline{D_{xx}}][\Phi]+[\Phi][\overline{D_{yy}}]\frac{1}{h^2}=0 \qquad (3-8)$$

with the real, symmetric and tridiagonal second order operators $[\overline{D_{xx}}]$ and $[\overline{D_{yy}}]$. A two fold discretized function is represented clearly by a two dimensional matrix. For the mathematical and computational solution of the boundary value problem, however, the representation of the discrete potential function in the form of a vector is more advantageous. Hence instead of eq.(3-8), the following equivalent equation is solved :

$$\frac{d^2}{dz^2}\vec{\Phi}+\frac{1}{h^2}[\overline{D_{xx}}]\vec{\Phi}+\frac{1}{h^2}[\overline{D_{yy}}]\vec{\Phi}=\vec{0} \qquad (3-9)$$

with the vector $\vec{\Phi}=(\vec{\Phi}_1,\ldots,\vec{\Phi}_M)'$ whose elements are the column vectors of the potential matrix $[\Phi]$.

The second order operators take the form of block matrices defined by

$$[\overline{D_{xx}}]=[I]_{M_y}\otimes[\overline{D_{xx}}] \qquad (3-10)$$

and

$$[\overline{D_{yy}}]=[\overline{D_{yy}}]\otimes[I]_{M_y} \qquad (3-11)$$

where $[I]_{M_y(M_x)}$ denotes the unit matrix of order $M_y(M_x)$ and the symbol "$\otimes$" designates the Kronecker product.

The potentials $[\Phi]_{i,k}$ are coupled and the decoupling is achieved by a real transformation of the operators $[\overline{D_{xx}}]$ and $[\overline{D_{yy}}]$.

By this, the operators of eq.(3-9) are transformed to the block diagonal structure of their eigenvalues; i.e,

$$[\hat{T}]^t[\overline{\overline{D}}_{xx(yy)}][\hat{T}] = -[\hat{X}_{x(y)}]^2 \qquad (3-12)$$

with the matrix of eigenvectors

$$[\hat{T}] = [T_y] \otimes [T_x] \qquad (3-13)$$

where

[Tx] and **[Ty]** are the eigenvector matrices for the operators of eq.(3-8).

The transformation of eq.(3-9) yields the following set of $M_x M_y$ ordinary differential equations :

$$\frac{d^2}{dz^2}\vec{\vec{\Phi}} - \left[\frac{\hat{X}_z}{h}\right]^2 \vec{\vec{\Phi}} = \vec{\vec{0}} \qquad (3-14)$$

where

$$\vec{\vec{\Phi}} = [\hat{T}]^t \vec{\Phi} \qquad (3-15a)$$

and

$$\left[\frac{\hat{X}_z}{h}\right]^2 = \left[\frac{\hat{X}_x}{h}\right]^2 + \left[\frac{\hat{X}_y}{h}\right]^2 \qquad (3-15b)$$

If **h** is not the same in **x** and **y** coordinates, we take the smallest of the two in order to guaranty the desired precision of calculation in both space directions **x** and **y**.

3-2-2 Interface continuity conditions:

Equation (3-14) is similar to eq.(2-18) and the solution is similar to the one given in eq.(2-19a). With the same steps as in section (2-3), matching the fields at the interfaces and using boundary conditions, we end up with a matrix relating the conductors electric potential vector to the electric charge vector in the following form :

$$\begin{bmatrix} \vec{\tilde{\Phi}}_A \\ \vec{\tilde{\Phi}}_B \end{bmatrix} = \begin{bmatrix} [\tilde{\Gamma}_{11}] & [\tilde{\Gamma}_{12}] \\ [\tilde{\Gamma}_{21}] & [\tilde{\Gamma}_{22}] \end{bmatrix} \begin{bmatrix} \vec{\tilde{Q}}_A \\ \vec{\tilde{Q}}_B \end{bmatrix} \qquad (3-16)$$

where the $[\tilde{\Gamma}_{mn}]$ are block diagonal matrices of order **Mx.My**.

3-2-3 Transformation in the original domain:

The transformed vectors of potentials and charges are related to the corresponding vectors in the original domain by:

$$\vec{\phi}_{A(B)} = [\hat{f}_e][\hat{T}]\vec{\tilde{\Phi}}_{A(B)} \qquad (3-17)$$

and

$$\vec{q}_{A(B)} = [\hat{f}_e]^{-1}[\hat{T}]\vec{\tilde{Q}}_{A(B)} \qquad (3-18)$$

with

$$[\hat{r}_e] = [r_{e_y}] \otimes [r_{e_x}] \qquad (3-19)$$

3-2-4 Determination of conductors coupling capacitance:

After doing the inverse transformation of eq.(3-16) into the original domain and after the inversion of the reduced matrix, one obtains the following equation :

$$\vec{q}_{red} = [\gamma]^{-1}_{red} \vec{\phi}_{red} = [C]\vec{\phi}_{red} \qquad (3-20)$$

Where [C] is the microcapacitance matrix. The macro or conductor capacitances are calculated by partitioning [C] and summing up the appropriate terms, (see Appendix B). This yields:

$$\vec{q}_{cond} = \begin{bmatrix} C_{11} & C_{12} \\ C_{21} & C_{22} \end{bmatrix}_{cond} \vec{\phi}_{cond} \qquad (3-21)$$

where C_{12} and C_{21} are equal and represent the lumped coupling capacitance between conductors A and B.

3-3 MoI applied to discontinuities.

The MoL is applied to the capacitance calculation of arbitrary shaped metalization involving discontinuities by following, mainly, the steps of section (3-2) with a slight difference concerning the lateral walls, discretization pattern and matrix reduction that depend on the conductor shape. In the case of finite dimension metalization, electric lateral walls are used (Dirichlet-Dirichlet). Also, the dimension of the system of continuity equations depends on the number of dielectric interfaces containing, eventually many microstrip sections which is the case for couplers, filters and gap in microstrips ...etc. In this situation, similarly to sections (2-3), (3-2), a capacitance matrix is reached yielding the coupling and intrinsic capacitances.

3-4 The Method of Lines applied to anisotropic dielectrics.

For anisotropic dielectric substrates having diagonal tensor permitivity of form:

$$\bar{\epsilon} = \begin{bmatrix} \epsilon_x & 0 & 0 \\ 0 & \epsilon_y & 0 \\ 0 & 0 & \epsilon_z \end{bmatrix}$$

Laplace's equation ,from **[38]**,becomes:

$$\epsilon_x \frac{\partial^2 \phi}{\partial x^2} + \epsilon_y \frac{\partial^2 \phi}{\partial y^2} + \epsilon_z \frac{\partial^2 \phi}{\partial z^2} = 0 \qquad (3-22)$$

The MoL is applied as shown in sections (2-3),(3-2) for capacitance calculations by transforming (2-18) into:

$$\frac{d^2 V}{dy^2} - \frac{\epsilon_x}{\epsilon_y}\left(\frac{X}{h}\right)^2 V = 0 \qquad (3-23)$$

for constant cross-section structures, and eq.(3-14) into:

$$\frac{d^2}{dz^2}\vec{\Phi} - \left(\frac{\hat{X}_z}{h}\right)^2 \vec{\Phi} = \vec{0} \qquad (3-24)$$

with

$$\left(\frac{\hat{X}_z}{h}\right)^2 = \frac{\epsilon_x}{\epsilon_z}\left(\frac{\hat{X}_x}{h}\right)^2 + \frac{\epsilon_y}{\epsilon_z}\left(\frac{\hat{X}_y}{h}\right)^2 \qquad (3-25)$$

for three-dimensional problems with two-dimensional discretization.

3-5 Software description.

As shown in Fig.3-3, the software program runs as follows:

1-The user inputs the structure dimensions in **x** and **y** directions as well as the dielectric substrate thicknesses and permitivities

2-The smallest interval size Δ and the scaling factor **h** are calculated and the smallest values are selected between the **x-y** directions from (eqs.2-32, 2-33).

3-The discretization is performed as explained in section (2-3-5) as long as the conductors have finite dimensions in **x-y** directions. However, when they have infinite lengths (crossing conductors), Neumann's conditions are used by centering the lateral walls between two consecutive equi-potential lines. The edge conditions are considered as explicited in section(2-3-5). The dicretization leads to the intervals $h_{t_x}, h_{t_y}, e_{t_x}, e_{t_y}$ and their respective numbers **Mx**, **My**.

4-The normalization matrices $r_{h_x}, r_{h_y}, r_{e_x}, r_{e_y}$ are constructed from eqs.(3-6), (3-7).

5-The second order difference operator **Dx**, **Dy** are constructed using (eq.2-7) for finite dimension conductors and (eq.3-3) for infinitely long conductors.

6-The matrices $\overline{Dxx}, \overline{Dyy}$ are determined using (eq.3-4).

7-The matrix pattern of the electric potential is converted, for computational convenience, in vector form by using Kronecker product and transforming the matrices $\overline{Dxx}, \overline{Dyy}$ in $\overline{Dxx}, \overline{Dyy}$ using (eqs.3-10, 3-11).

8-The eigenvector matrices **Tx**, **Ty** of $\overline{Dxx}, \overline{Dyy}$ are obtained from the QL algorithm.

9-The eigenvector matrix $\hat{T}$ is calculated from (eq.3-13).

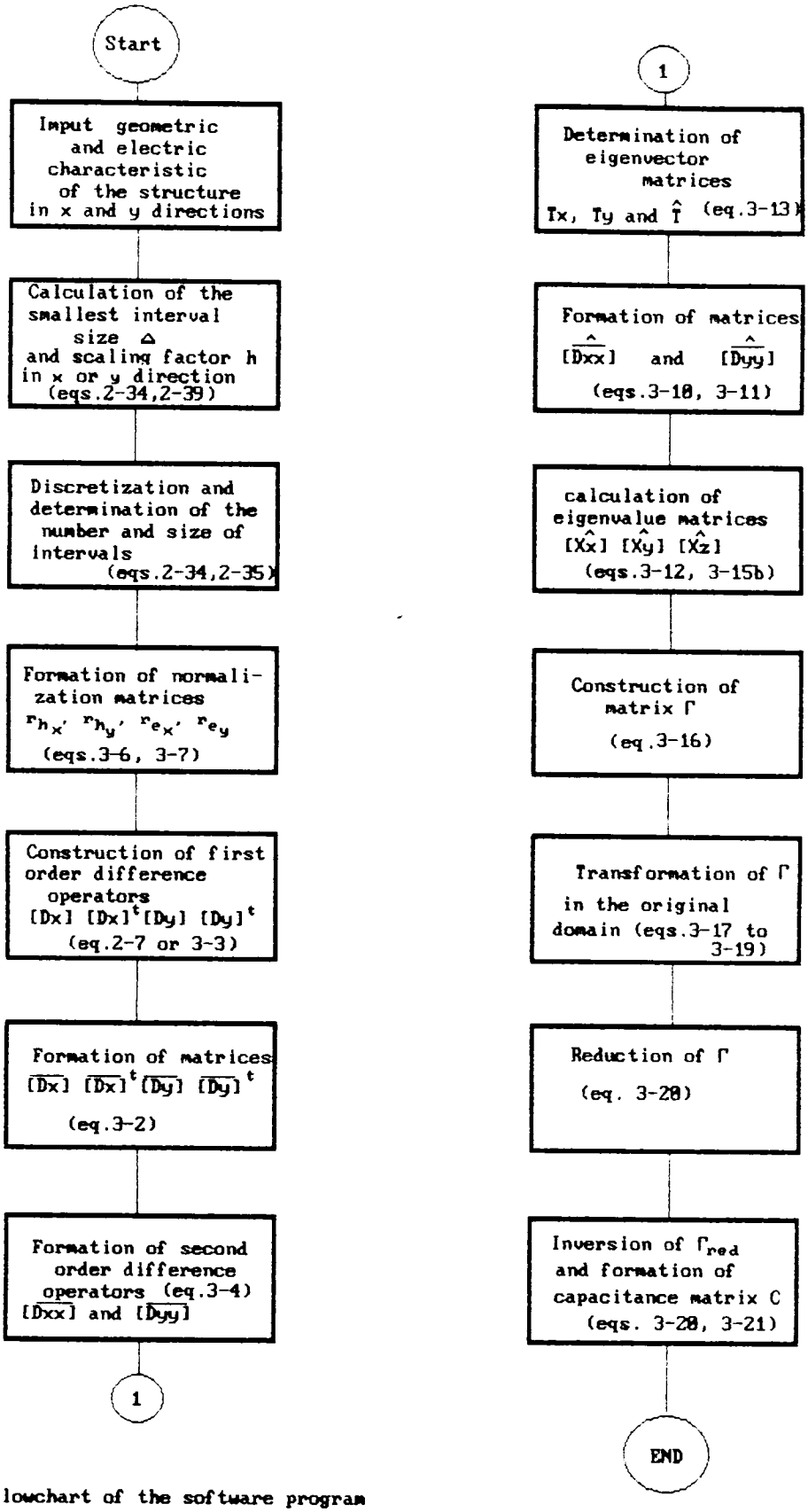

Fig.3-3. Flowchart of the software program using two-dimensional discretization.

10-The eigenvalue matrices of $\overline{Dxx}, \overline{Dyy}$ $(-(\hat{X}_x)^2, -(\hat{X}_y)^2)$ are calculated by (eq.3-12).

11-The eigenvalue matrix $(-(\hat{X}_z)^2)$ is determined from (eq.3-15b).

12- A system of equations similar to (eqs.2-20, 2-21) is solved to construct the matrix Γ relating the electric and charge vectors using (eq.3-16).

13-The matrix Γ is transformed in the original domain using (eqs.3-17, 3-18, 3-19)

14-This matrix in the original domain is reduced to the non-zero elements of the electric charge vector using (eq.3-20), (see fig.2-4).

15-The reduced matrix is inverted and summed up appropria-tely (see appendixB) to obtain the capacitance matrix using (3-20). For crossing conductors, the off-diagonal elements correspond to the coupling capacitance (eq.3-21).

3-6 Conclusion.

In this chapter, it has been shown how the MoL is suitable to deal with complex structures such as crossing conductors and microstrip sections having eventually anisotropic dielectric substrates. The analysis may be extended to multiple crossing interconnections as well as to multiple finite dimension metalizations at different interfaces. The computational power of this method is exhibited in the next chapter by comparing the MoL results to those obtained with other techniques that involve more complexe mathematical approaches.

CHAPTER4

RESULTS AND DISCUSSION.

In this chapter, the results obtained with the software programs written in FORTRAN 77 on MICROVAX II, based on the MoL, are compared to previous published data where other analytical and numerical techniques have been used. In the first section, one variable discretization is considered with the study of the shielding effects and the determination of some TEM parameters for few structures. In section two, two-variable discretization is applied to crossing conductors and some microstrip sections and discontinuities. The anisotropy effects of Sapphire are investigated for all the structures.

4-1 Constant cross-section structures:

The developed software based on the MoL in quasi-static approach, can be applied to parallel microstrips MIC interconnections occurring either as one or two layers of N conductors located at the interfaces of isotropic/anisotropic dielectric substrates, (Fig.2-2). This program can be used as a CAD tool to optimize the MIC interconnections positions to maximize or minimize, depending on the application, the TEM paramaters. The structures are considered with constant cross section; i.e. with conductors lengths very large compared to their widths.

4-1-1 Effects of shielding walls:

The closed enclosure composed of top and bottom conducting planes as well as lateral electric walls, (Fig.2-2) is necessary for our analysis with the MoL. The bottom ground plane is part of the microstrip structure, however the top plane and lateral walls do not exist when open structures are considered. Hence their effects on the lineique capacitance of a microstrip have been studied. In Fig.4-1, the influence of the distance **H1** between the top plane and the strip on the capacitance is shown for permitivities 1, 16 and strip widths 0.1 and 1. We can see that, as predicted, the effects of the upper shielding plane on the capacitance are more accentuated for lower substrate permitivities and wider strips.

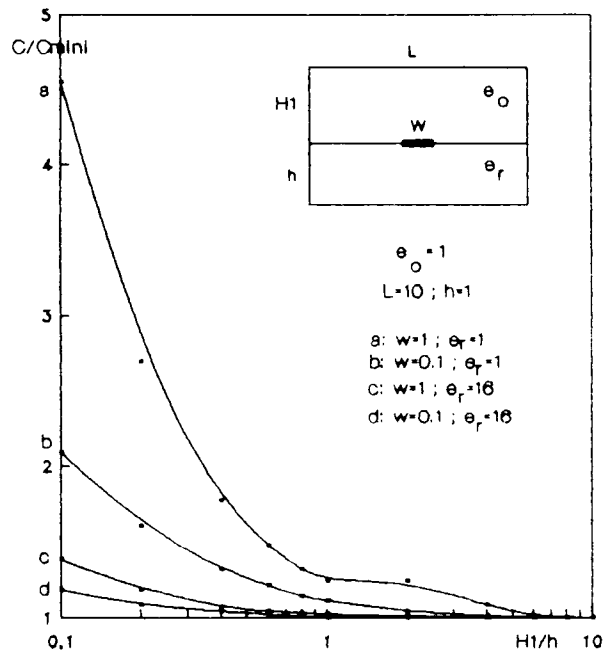

Fig.4-1. Effects of the top wall on the microstrip capacitance.

In Fig.4-2, the capacitance is sketched versus **L/h** (lateral walls distance normalized with respect to the substrate thickness) for permitivities 1,16, strip width **w**=1 , substrate thickness h=1 and top plane distance **H1**=0.1 and 10. We notice, as predicted, that the lateral walls distance affects more the microstrip capacitance for lower permitivities and farther top plane.

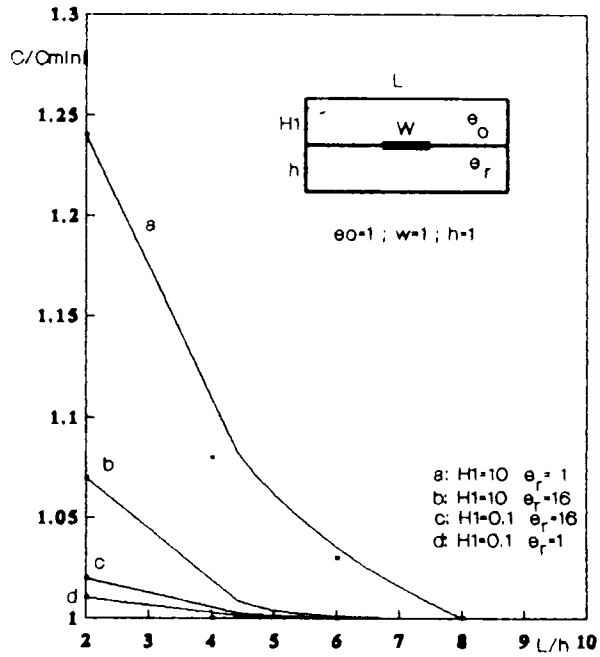

Fig.4-2. Effects of the lateral walls distance on the microstrip capacitance.

Finally, from Figs.(4-1) and (4-2), we conclude that, as long as both **L/h** and **H1/h** are greater than 10, the structures behave as quasi-open. These conditions will be used further to compare our results to published data where open structures have been considered.

4-1-2-1 Convergence rates.

The MoL is compared to an analytical technique (Green's function integral equation technique) which was applied by Kammler [18] who considered parallel conductors with vanishing thickness, placed between infinite perfectly conducting planes. In Fig.4-3, the methods are compared for the convergence rate and we can see that the MoL reaches 1 % error with less numerical efforts than the IET.

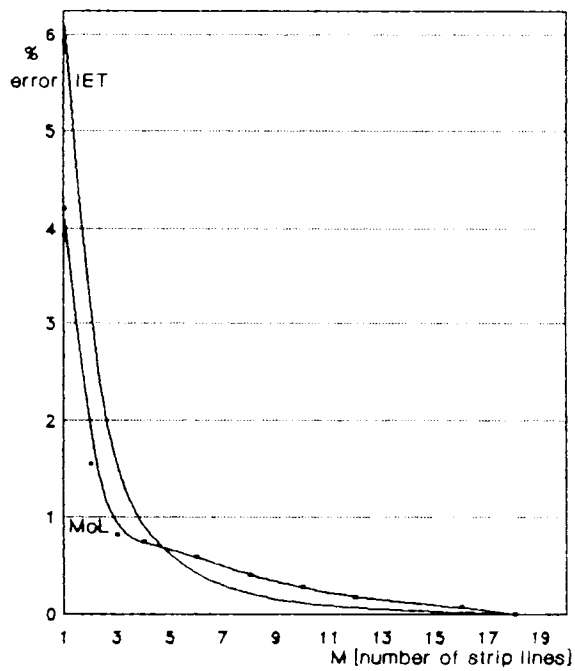

Fig. 4-3 Convergence rates of MoL and IET.

4-1-2-2 Capacitance matrices of multistrip structures.

The two methods are compared by considering different structures (Fig.4-4).

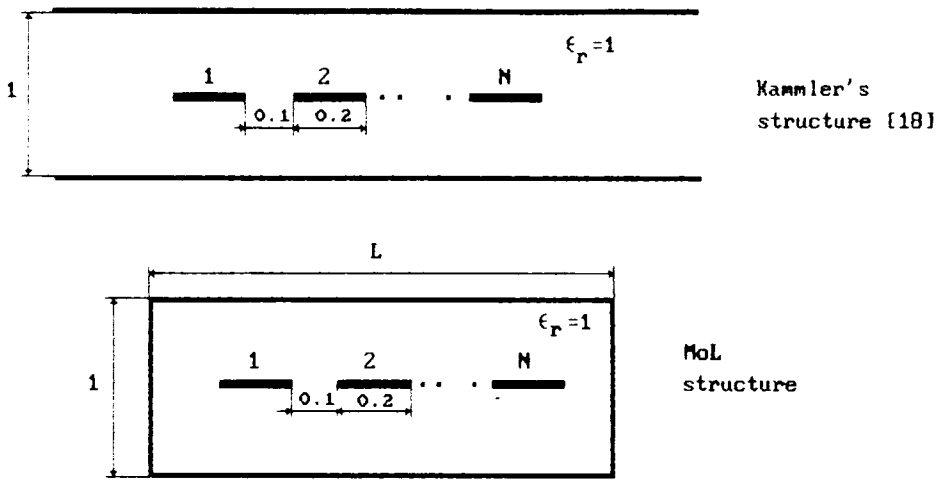

Fig.4-4. Cross-section of a multistrip structure.

In tables 4-1 to 4-5 , the intrinsic and mutual capacitances are compared by considering only the diagonal and subdiagonal elements of the symmetric capacitance matrices. For the largest structure (N=5), the capacitance matrix converges with an accuracy of 0.3 % in 5 seconds.

TABLE 4-1 For N=1

	MoL	Kammler	Difference δ
C/eo pf/m	2.4768	2.4618	0.60

TABLE 4-2

For N=2

	MoL	Kammler	Difference %
C11	2.9045	2.8888	0.54
C12	-1.0457	-1.0379	0.74

C11 = C22
C12 = C21

TABLE 4-3

For N=3

C/eo	MoL	Kammler	Difference %
C11	2.9071	2.8914	0.54
C22	3.3076	3.2915	0.47
C12	-1.0139	-1.0064	0.74
C13	-0.0846	-0.0841	0.59

C11 = C33
C12 = C21 = C23 = C32
C13 = C31

TABLE 4-4

For N=4

C/eo	MoL	Kammler	Difference %
C11	2.9072	2.8914	0.54
C22	3.3098	3.2938	0.48
C12	-1.0135	-1.0061	0.73
C23	-0.9839	-0.9767	0.73
C13	-0.0799	-0.0795	0.50
C14	-0.0125	-0.0125	0.00

C11=C44 ; C22=C33 ; C12=C21=C34=C43
C23=C32 ; C13=C31=C24=C42 ; C14=C41

TABLE 4-5 For N=5

C/eo	MoL	Kammler	Difference %
C11	2.9072	2.8914	0.54
C22	3.3099	3.2939	0.48
C33	3.3120	3.2961	0.48
C12	-1.0135	-1.0061	0.73
C23	-0.9835	-0.9764	0.72
C13	-0.0799	-0.0794	0.62
C24	-0.0755	-0.0751	0.53
C14	-0.0118	-0.0117	0.85
C15	-0.0020	-0.0020	0.00

C11=C55 ; C22=C44 ; C12=C21=C45=C54
C23=C32=C34=C43 ; C13=C31=C35=C53
C24=C42 ; C14=C41=C25=C52 ; C15=C51

Our software program for two layers of parallel multistrips is applied to a structure that has been analyzed by Kammler [18] (Fig.4-5).

In table 4-6, our results are compared to those of Kammler and they show a very good agreement. The percentage difference does not exceed 0.4 % within an accuracy of 0.8 % and a computation time of 7 seconds.

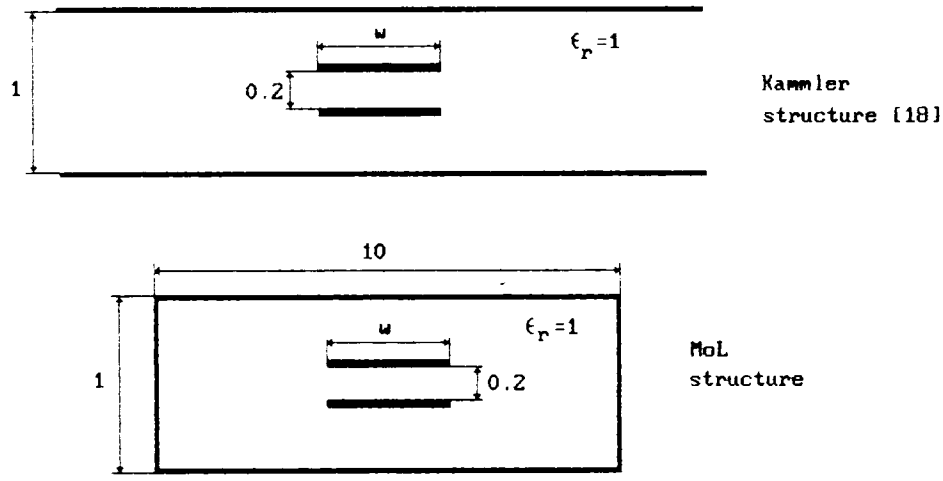

Fig.4-5. A two layer monostrip structure.

TABLE 4-6

C/W	W=0.6			W=1		
C/eo	MoL	Kammler	Dif.%	MoL	Kammler	Dif.%
C11	6.157	6.134	0.37	9.166	9.136	0.33
C12	-3.0366	-3.0364	0.36	-5.369	-5.355	0.26

C11=C22
C12=C21

4-1-3 Capacitance matrix of two layers of three conductors.

The capacitance matrix is determined for two layers of three conductors separated by a dielectric of permitivity 11.6 as

shown in Fig.4-6.

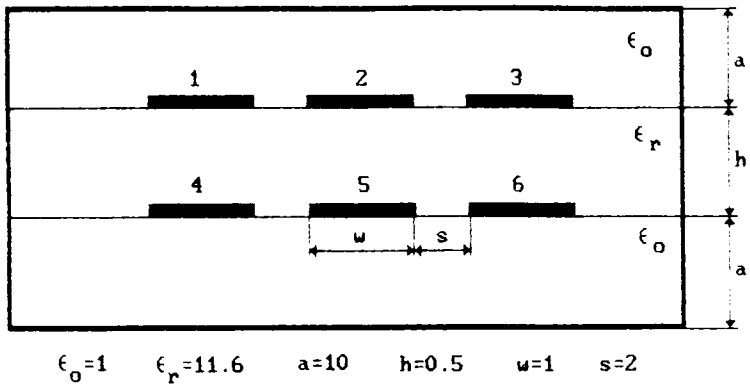

Fig.4-6. Cross-section of a two layer three conductor structure.

The capacitance matrix obtained in 1 min of computations with an accuracy of 1.5 %, is:

$$\frac{C}{\epsilon_o} = \begin{bmatrix} 31.34 & 0.86 & 0.06 & 28.67 & 0.80 & 0.05 \\ 0.86 & 31.86 & 0.86 & 0.80 & 28.16 & 0.80 \\ 0.06 & 0.86 & 31.34 & 0.05 & 0.80 & 28.67 \\ 28.67 & 0.80 & 0.05 & 31.34 & 0.86 & 0.06 \\ 0.80 & 28.16 & 0.80 & 0.86 & 31.86 & 0.86 \\ 0.05 & 0.80 & 28.67 & 0.06 & 0.86 & 31.34 \end{bmatrix} pF/m$$

We remark, as predicted, that the matrix elements with the highest values correspond to the diagonal elements, representing the intrinsic capacitances, and to the coupling capacitances between superposed conductors (elements C_{14};C_{41};C_{25};C_{52};C_{36} and C_{63}). We notice, also, the smallest capacitance values C_{16};C_{61};C_{34} and C_{43}) which are the coupling between the most distant conductors: (1 and 6) and (3 and 4).

4-1-4 TEM parameters of microstrips for some isotropic and anisotropic dielectrics.

The TEM parameters have been determined for different isotropic and anisotropic dielectric substrates and sketched with respect to W/h. We obtained an accuracy of 0.3 % in 1 second for each point.In order to compare our results to those of T.C.Edwards [21], we took a Sapphire substrate with permitivity tensor along x,y,z directions (10.6; 11.6; 10.6). From Fig.4-7, it is noticeable that the permitivity effects decrease for smaller values of W/h and that the capacitance is more affected, by the ratio W/h, for higher substrate permitivities and higher W/h ratios. Similar remarks can be done for the impedance as expected from its inverse proportionality relation with capacitance. The impedance curve for Sapphire agrees well with the results of T.C.Edwards [1, 21] who used finite difference method.

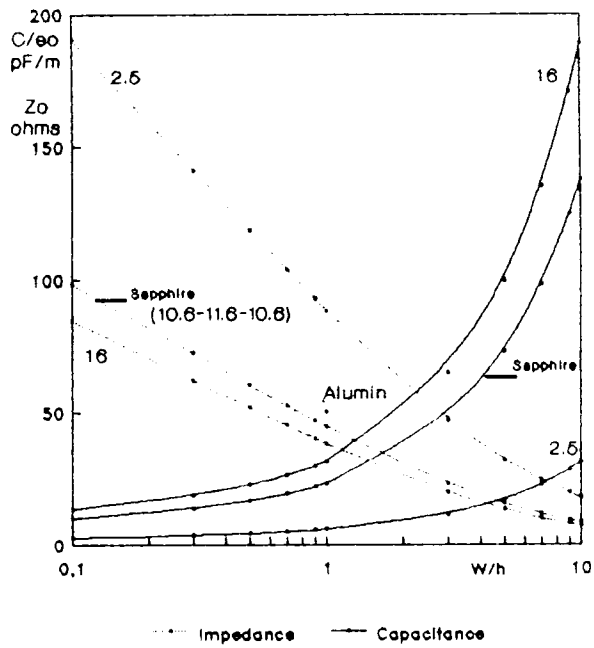

Fig. 4-7 Impedances and capacitances of some isotropic and anisotropic dielectric substrates.

The effective permitivity curves are illustrated in Fig.4-8.

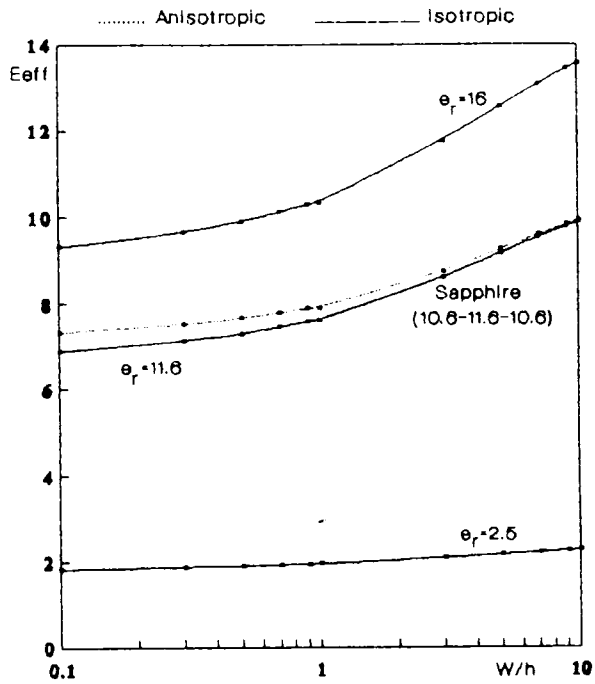

Fig. 4-8 Effective permitivities of some isotropic and anisotropic dielectric substrates.

For a Sapphire substrate, our results agree very well with those of T. C. Edwards **[1, 21]**. As predicted, we notice that the anisotropy effects increase for smaller **W/h** and that the effective permitivity is less affected by **W/h** for smaller permitivities.

4-2 Some three-dimensional problems.

A software program, based on the MoL in quasi-static approach, has been developed for capacitance calculation concerning structures having discontinuities in both **x** and **y**

directions and involving two-dimensional discretization. This program has been applied to two isolated crossing conductors, rectangular microstrips and to the determination of the fringing capacitance of an open-end microstrip with isotropic and anisotropic dielectrics.

4-2-1 Coupling capacitance of two crossing conductors:

In MMIC's and MIC's, it happens frequently that the interconnections cross orthogonally at different dielectric interfaces such as bridges and underpasses in which the coupling is predominantly capacitive. We have applied our program to determine and study the coupling capacitance of two crossing conductors separated by isotropic and anisotropic dielectrics.

4-2-1-1 Effect of lateral walls.

We have studied the magnetic walls distance effects on the coupling capacitance as shown in Fig.4-9.

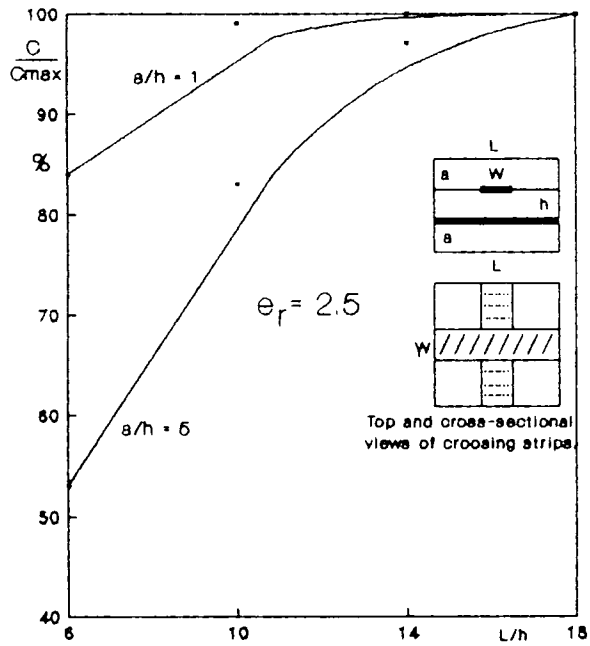

Fig. 4-9 Effect of the lateral walls on the coupling capacitance of two crossing conductors.

We can see from this figure that for a given substrate thickness **h** and more distant top plane, the magnetic lateral walls distance has to be increased to neglect their effect and determine the actual coupling capacitance.

4-2-1-2 Effect of substrate thickness and anisotropy:

We have studied the influence of substrate thickness on the coupling capacitance for different conductors widths with isotropic and anisotropic (Sapphire) dielectrics. For permitivity 3.8, the results obtained within an accuracy of 2 %, agree well with those published by Veit et al.**[16]**. In Fig.4-10, we notice that as the strip width increases, the coupling capacitance goes through a minimum for thinner substrates. This avoids the designers the use of prohibitive substrate thicknesses that may be needed in order to reduce the coupling capacitance when it is undesired. We remark also, that the anisotropy effects are more important for thicker substrates.

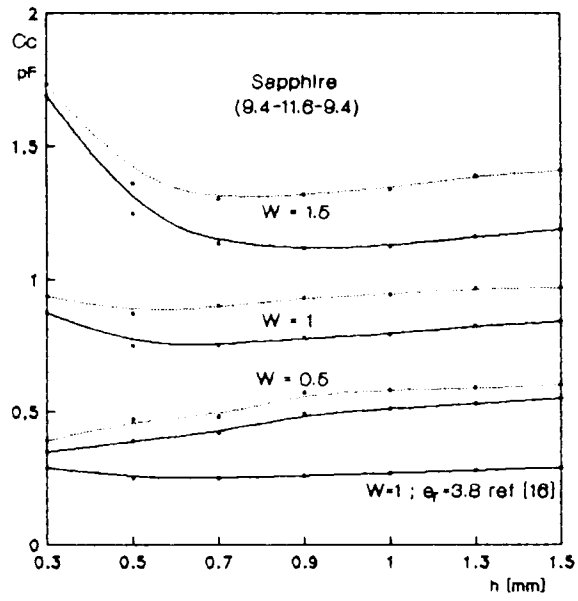

Fig. 4-10 Effect of Sapphire substrate thickness on the coupling capacitance of two crossing conductors.

4-2-2 Capacitance of rectangular microstrips:

We have determined the capacitance of rectangular microstrips with different shapes and isotropic/anisotropic substrates, (Fig.4-11).

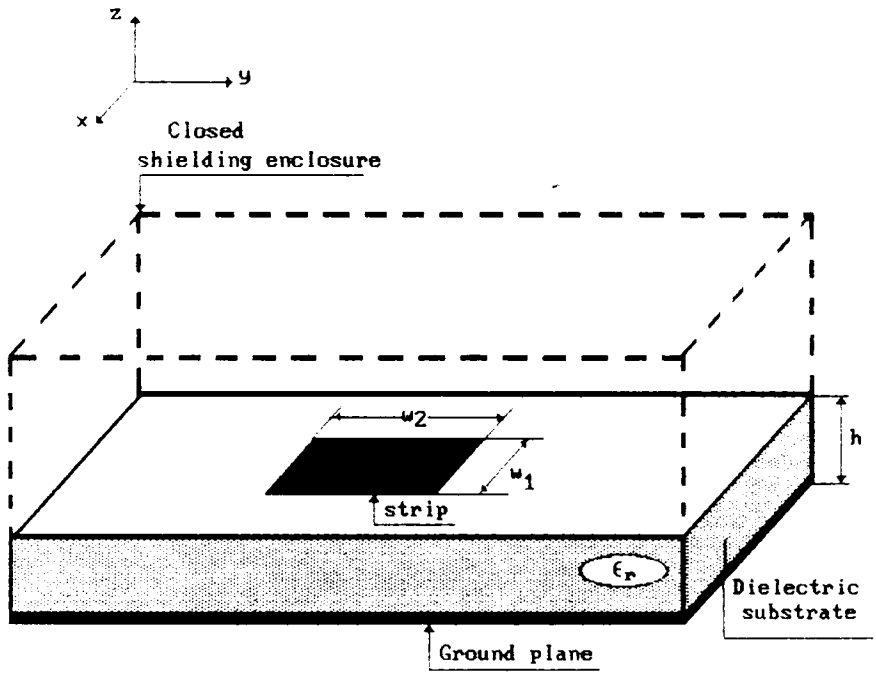

Fig.4-11. A rectangular microstrip ($w_1 \times w_2$) deposited on a dielectric substrate of permitivity ϵ_r and thickness h.

A dielectric substrate with permitivity 1 was considered for microstrip length to width ratios of 1 and 0.2 in order to compare our results to previous published data. Also, a

sapphire substrate, with the previous microstrip dimensions ratios, has been used in both isotropic (ϵ_r=11.6) and anisotropic cases (ϵ_x=9.4;ϵ_y=9.4;ϵ_z=11.6) to illustrate the anisotropy effect on discontinuity capacitances. The normalized capacitance with respect to $\epsilon_r\epsilon_o\frac{W_1W_2}{h}$ (the capacitance of two parallel plates having dimensions W_1xW_2 separated by a dielectric substrate of thickness **h**), is sketched in Fig.4-12, with respect to the ratio **h/W1**. An accuracy of 1.7 % is ashieved in 41 min of computations, for each point.

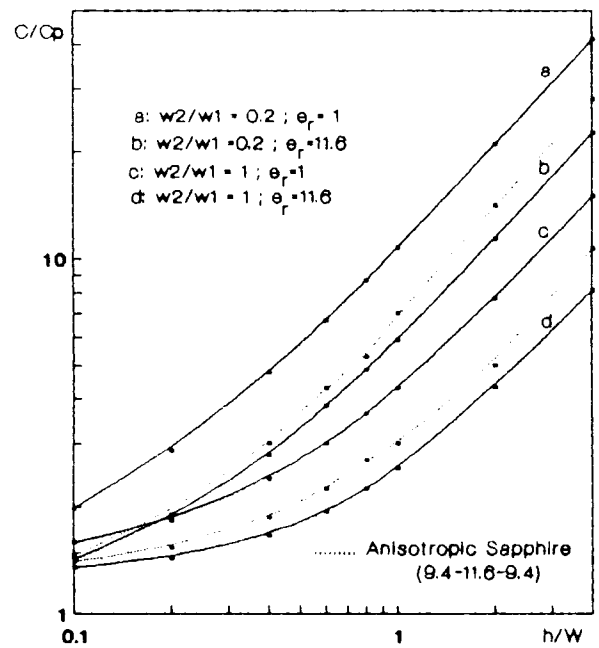

Fig. 4-12 Normalized capacitances of rectangular microstrip sections.

As predicted, the microstrip capacitance approaches the parallel plate capacitance for smaller values of **h/W** and

faster for a larger microstrip area. Our curves are very similar to those obtained by T.Itoh et al. who employed Galerkin's method in spectral domain [10], and to those published by A.Farrar et al. who used a Green's function matrix method [11]. As remarked previously, we notice that the anisotropy effect, for Sapphire, increases with higher values of h/W1.

4-2-3 Open-end microstrip capacitance

The fringing capacitance at the end of a microstrip line may be defined, as given in [10], by:

$$\lim_{l\to\infty}\frac{1}{2}[C(l)-lCo] \qquad (4-1)$$

where C(1) is the total capacitance of the section of length 1 and width W, Co is the lineique capacitance of a uniform infinitely long line of the same width, and the factor 1/2 accounts for the discontinuities at both ends of the strip. In the calculations, 1 is not infinite, but some finitely large value compared to the width beyond which the change of [C(1) - 1Co] is negligible. We have taken 1=5W and the obtained results are very close to those of P. Sylvester et al. [12] who applied a Green's function integral equation technique. In Fig.4-13, the open end fringing microstrip capacitance normalized with respect to the strip width, is sketched versus W/h for isotropic dielectrics (ϵ_r=2.5;16;11.6) and an anisotropic substrate of Sapphire (ϵ_x=9.4;ϵ_y=9.4;ϵ_z=11.6). For each point an accuracy of 2.8 % is obtained with 53 min of computations. We notice that both the fringing capacitance and its rate of

variation with W/h decreases for higher values of W/h which agrees with theoretical predictions. In this case also, the anisotropy effects increase with smaller values of **W/h**.

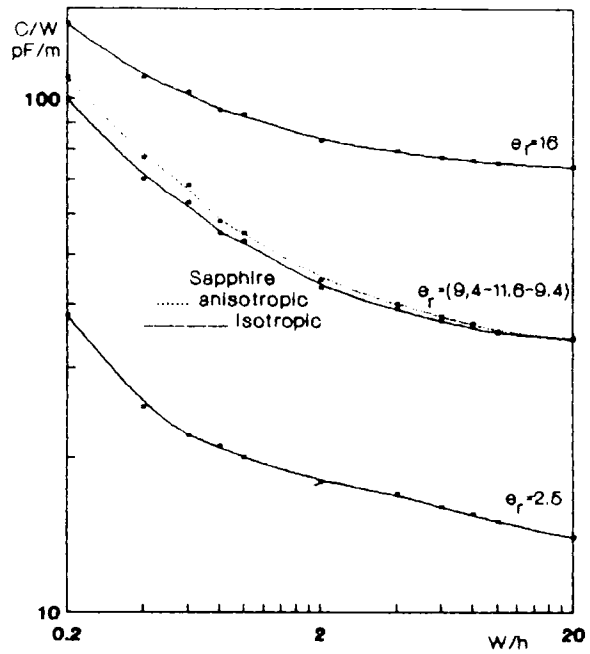

Fig. 4-13 Fringing capacitances of open end microstrips.

4-3 Conclusion:

The MoL, necessiting in quasi-static mode a shielding enclosure, can give accurate results for capacitances, impedances and effective permitivities that have to be determined for open structures. Also, this method handles, elegantly, complexe two- and three-dimensional problems such as multilayer parallel multistrip structures, crossing conductors, microstrip rectangular sections and open-end discontinuities with both isotropic and anisotropic dielectric substrates.

CONCLUSION

The method of lines, in quasi-static approach, has been applied to develop a software program for the analysis of MIC and MMIC structures in two and three dimensions.

We have started with the determination of the conditions in which the shielding enclosure has negligible effects on the conductors capacitances; simulating quasi-open structures. We have, also, extended the application of this method to two-layer multistrip structures, crossing conductors, microstrip rectangular sections and open-ends with anisotropic dielectrics.

All the results agree very well with theoretical predictions and published results obtained by other techniques involving much more complex approaches. We can confirm also, that the considered shielding dimensions yield results very close to those reached with open structures and that the MoL has a great suitability to deal with complex MIC two- and three-dimensional problems involving isotropic and anisotropic dielectric substrates.

Our software program may be used as a CAD tool to optimize the dielectric permitivity, the positionning of MIC interconnections as well as the sizes of the conductors, the dielectric substrates and the shielding.

However, we encountered memory space and computing time problems with thick dielectric substrates. Hopefully, the Method of Lines is being extended to deal with absorbing boundaries and this will reduce considerably the analyses computing efforts.

This method should be extended not only to more complex microstrip discontinuities for the capacitance modeling of the charges excess occuring at the metalization corners and abrupt changes in width, but also to hybrid mode approach for more accurate analyses.

REFERENCES

[1] T. C. EDWARDS.
" Foundations for microstrip circuits and design."
John Wiley & sons, 1981.

[2] K. C. GUPTA, R. GARG, I. J. BAHL.
" Microstrip lines and slotlines."
Artech. House Inc., Massachussets USA., 1979.

[3] P. WALDOW.
" A simulation tool for multiconductor coupled lines.",
Microwave and RF engineering, pp 27-33, Nov/Dec 1989.

[4] J. A. WEISS.
" Microwave propagation on coupled pairs of microstrip transmission lines," in advances in microwaves.
New York: Academic, vol. 8, 1974, pp 295-320.

[5] H. A. WHEELER.
" Transmission line properties of parallel strips separated by a dielectric sheet," IEEE Trans. Microwave Theory Tech., vol. MTT-13, pp 172-185, Mar 1965.

[6] E. YAMASHITA.
" Variational method for the analysis of microstrip-like transmission lines , " IEEE Trans. Microwave Theory Tech. vol. MTT-16, pp 529-535, Aug 1968.

[7] R. MITTRA and T. ITOH.
" Charge and potential distributions in shielded striplines , " IEEE Trans. Microwave Theory Tech., vol MTT-18, pp. 149-156, Mar 1970.

[8] A. FARRAR and A. T. ADAMS.
" Computation of propagation constants for the fundamental and higher order modes in microstrip, " IEEE Trans. Microwave Theory Tech., vol. MTT-24, pp. 456-460, July 1976.

[9] T. ITOH.
" Generalized spectral domain method for multiconductor printed lines and its application to turnable suspended microstrips, " IEEE Trans. Microwave Theory Tech., vol MTT-26, pp. 983-987, Dec.1978.

[10] T. ITOH, R. MITTRA and R. D. WARD.
" A method for computing edge capacitance of finite and semi-infinite microstrip lines," IEEE Trans. Microwave Theory Tech., pp 847-849, Dec 1972.

[11] A. FARRAR, A. T. ADAMS.
" Matrix methods for microstrip three-dimensional problems" IEEE Trans. Microwave Theory Tech., vol. MTT-20, No. 8., pp 497-504, August 1972.

[12] P. SILVESTER and P. BENEDEK.
" Equivalent capacitances of microstrip open circuits, " IEEE Trans. Microwave Theory Tech., vol. MTT-20. No. 8., pp 511-516, August 1972.

[13] U. SCHULZ and R. PREGLA.
" A new technique for the analysis of the dispersion characteristics of planar waveguides, " AEU, Band 34, Heft 4, pp. 169-173, 1980.

[14] S. B. WORM and R. PREGLA.
" Hybrid-mode analysis of arbitrary shaped planar microwave structures by the method of lines, " IEEE Trans. Microwave Theory Tech., vol. MTT-32. No. 2., pp 191-196, Febrary 1984.

[15] H. DIESTEL.
" Analysis of planar multiconductor transmission-line systems with the method of lines, " AEU, Band 41, Heft 3, pp 169-175, 1987.

[16] W. VEIT, H. DIESTEL and R. PREGLA.
" Coupling of crossed planar multiconductor systems, " IEEE Trans. Microwave Theory Tech., vol. 38, No 3, pp 265-269, March 1990.

[17] B. BHAT and S. K. KOUL.
" Stripline-like transmission lines for microwave integrated circuits ", J. Wiley, 1989.

[18] D. W. KAMMLER.
" Calculation of characteristic admittances and coupling coefficients for strip transmission lines, " IEEE Trans. Microwave Theory Tech., vol. MTT-16, No.11, pp. 925-937, Nov. 1968.

[19] C. WEI, R. F. HARRINGTON and J. R. MAUTZ.
" Multiconductor transmission lines in multilayered dielectric media, " IEEE Trans. Microwave Theory Tech., vol.32, No. 4, pp 439-450, April 1984.

[20] H. G. BERGANDT and R. PREGLA.
" Calculation of the even- and odd-mode capacitance parameters for coupled microstrips, " AEU, vol.26, pp. 153-158, 1972.

[21] R. P. OWENS, J. E. AITKEN and T. C. EDWARDS.
" Quasi-static characteristics of microstrip on an anisotropic sapphire substrate, " IEEE Trans. Microwave Theory Tech., vol. MTT-24, No. 8, pp 499-505, August 1976.

[22] **V. K. TRIPATHI and R. J. BOCOLO.**
" A simple network analog approach for the quasi-static caracteristics of general lossy, anisotropic, layered structures, " IEEE Trans. Microwave Theory Tech., vol. MTT-33, No. 12, pp 458-464, Dec. 1985.

[23] **B. L. LENNARTSSON.**
" A network analog method for computing the TEM caracteristics of planar transmission lines," IEEE Trans. Microwave Theory Tech., vol. MTT-20, No.9, pp 586-591, Sept 1972.

[24] **S. M. SAAD.**
" Review of numerical methods for the analysis of arbitrary shaped microwave and optical dielectric waveguides, " IEEE Trans. Microwave Theory Tech., vol. MTT-33, No. 10, pp 894-899, Oct 1985.

[25] **R. PREGLA.**
" Calculation of the distributed capacitances and phase velecities in coupled microstrip lines by conformal mapping techniques, " AEU, vol. 26, pp. 470-474, 1972.

[26] **D. MIRSHEKAR-SYAHKAL.**
" Spectral domain method for microwave integrated circuits ", J. Wiley & sons INC., 1990.

[27] **V. F. FUSCO.**
" Microwave circuits analysis and computer-aided design ", PHI, 1987.

[28] **O. A. LISKOVETS.**
" The method of lines," Review, Differential'nye Uravneniya, vol. 1, No. 12, pp. 1662-1678, 1965.

[29] **U. SCHULZ.**
" On the edge condition with the method of lines in planar waveguides, " AEU 34 [1980], 176-178.

[30] **R. PREGLA and W. PASCHER.**
" The Method of Lines," in numerical techniques for microwave and millimeter wave passive structures, T. Itoh, ed., (J. Wiley, Newyork, 1989), Chap. 6, pp. 381-446.

[31] **J. H. MATHEWS.**
" Numerical Methods for Mathematics, Science, And Engineering ", 2nd edition, PHI-Editions, 1992.

[32] **G. DAHLQUIST.**
" Numerical methods", in Automatic Computation, PHI, INC., New Jersey, pp. 157-159, 1974.

[33] **J. C. MAXWELL.**
" A threatise on electricity and magnetism, " 3rd ed., vol. 1. New York: Dover, 1954, pp. 296-297.

[34] L. WIEMER and R. H. JANSEN.
" Determination of coupling capacitance of underpasses, air bridges and crossings in MIC's and MMIC's, " Electron. Lett., vol. 23, No. 7, pp. 344-346, 1987.

[35] T. UWANO, R. SOPRRENTINO and T. ITOH.
" Characterization of strip line crossing by transverse resonance analysis, " IEEE Trans. Microwave Theory Tech., vol.MTT-35, pp. 1369-1376, Dec 1987.

[36] M. MAEDA.
" An analysis of gap in microstrip transmission lines, " IEEE Trans. Microwave Theory Tech., vol. MTT-20, No. 6, pp 391-397, June 1972.

[37] A. E. RUEHLI and P. A. BRENNAN.
" Efficient capacitance calculations for three-dimensional multiconductor systems, " IEEE Trans. Microwave Theory Tech., vol. MTT-21, No.2, pp 76-82, Feb 1973.

[38] A. G. KEEN, M. J. WALE, M. I. SOBHY and A. J. HOLDEN.
" Quasi-static analysis of electrooptic modulators by the method of lines, " Journal of lightwave technology, vol.8, No. 1, pp 42-50, Jan 1990.

[39] M. AFFANE , A. OUADI and H. BOURDOUCEN
" Quasi-static analysis of integrated circuits para--llel interconnections", JETA conference, TUNISIA, 1992.

[40] M. AFFANE and H. BOURDOUCEN.
" Quasi-static analysis of hybrid and monolithic integra-ted circuits interconnections ", 43rd Electronic Compo-nents and Technology Conference, Orlando, Florida, USA, pp 1055-1060, June 3-5 1993.

[41] A. ISSAOUN.
" A quasi-static analysis of MMIC' transmission-line stru-ctures by the Method of Lines ", Magister thesis, No 01\92, INELEC, BOUMERDES, ALGERIA.

[42] L. BOUKBIR.
" Etude et développement d'analyseurs éléctromagnétiques pour circuits intégrés monolithiques et hybrides dans la bande millimétrique à partir de la méthode des lignes ", Doctoral thesis, No D92-13, INSA, RENNES, FRANCE.

APPENDIX A

LAPLACE'S EQUATION DERIVATION:

From Maxwell's equations,

$$\nabla . E = \rho \qquad (A-1)$$

where ∇ is the differential vector operator:

$$\frac{\partial}{\partial x}\hat{x} + \frac{\partial}{\partial y}\hat{y} + \frac{\partial}{\partial z}\hat{z} \qquad (A-2)$$

E is the electric field and ρ the electric charge density. As E is a gradient of an electric potential V,

$$E = -\nabla V \qquad (A-3)$$

leading to Poisson's equation:

$$\nabla . \nabla V = \nabla^2 V = \rho \qquad (A-4)$$

.

Since the electric potential is evaluated in dielectric substrates where $\rho = 0$, then the electric potential satisfies Laplace's equation given by:

$$\frac{\partial^2 V}{\partial x^2} + \frac{\partial^2 V}{\partial y^2} + \frac{\partial^2 V}{\partial z^2} = 0 \qquad (A-5)$$

or

$$\nabla^2 V = 0 \qquad (A-6)$$

APPENDIX B

SUMMATION OF MICROCAPACITANCE ELEMENTS:

Consider a strip conductor **k** whose width is discretized by **p** lines leading to an electric charge vector:

$$(q_{k_1}, q_{k_2}, \ldots, q_{k_p})^t$$

If the conductor **k** is at potential V_k, then the microcapacitance matrix C_{kk}, relating the conductor charge vector to potential vector, is as follows:

$$\begin{bmatrix} q_{k_1} \\ q_{k_2} \\ . \\ . \\ . \\ q_{k_p} \end{bmatrix} = \begin{bmatrix} C_{11} & C_{12} & . & . & . & C_{k_1 p} \\ . & . & . & . & . & . \\ . & . & . & . & . & . \\ . & . & . & . & . & . \\ . & . & . & . & . & . \\ C_{k_p 1} & C_{k_p 2} & . & . & . & C_{k_{pp}} \end{bmatrix} \begin{bmatrix} V_{k_1} \\ V_{k_2} \\ . \\ . \\ . \\ V_{k_p} \end{bmatrix} \qquad (B-1)$$

The intrinsic capacitance of the conductor is C_{kk} such that the conductor charge and potential are related by:

$$Q_k = C_{kk} V_k \qquad (B-2)$$

As the conductor potential is uniform, then (eq. B-2) yields:

$$\sum_{i=1}^{p} q_{k_i} = \left[\sum_{\substack{i=1 \\ j=1}}^{p} C_{k_{ij}} \right] V_k \qquad (B-3)$$

Hence, the intrinsic conductor capacitance is obtained by summing up the microcapacitance elements.

The mutual capacitance between conductors **m** and **n** (off-diagonal elements of capacitance matrix) is obtained by

considering the microcapacitance matrix relating the potential vector of conductor **m** and the charge vector of conductor **n** or inversly.

A N N E X E

[illegible] composition du jury en vue de la soutenance [illegible]

[illegible] ...Ingineerie.des.Systemes.Electroniques .

[illegible]r..AFFANE..Mahmoud......................................

SIDENT /: Mr B.HARRAOUBIA, Professeur. U.S.T.H.B

PORTEUR/: Dr H.BOURDOUCEN, Thèse unique, Maitre de Conferences INELEC

MBRES /: Dr.M.DJEDDI, Phd, Charge de Cours, I.N.E.L.E.C

Dr.M.ATTARI, Thèse unique, Charge de Cours, U.S.T.H.B